Effect of Unit Operations on Food Particles – Evaluated by image analysis and correlated with mechanical tests

Jan Roland Guerrero Molina and Nuti Hutasingh

DIVISION OF PACKAGING LOGISTICS | DEPARTMENT OF DESIGN SCIENCES
FACULTY OF ENGINEERING LTH | LUND UNIVERSITY
2019

MASTER THESIS

This Master's thesis has been done within the Erasmus Mundus
Joint Master Degree FIPDes, Food Innovation and Product Design.

Jan Roland Guerrero Molina and Nuti Hutasingh

LUND
UNIVERSITY

Effect of Unit Operations to Food Particles – Evaluated by Image Analysis and Correlated with Mechanical Tests

Abstract

In order to successfully produce food products containing less damaged particles (approx. 1 cm^3) it is important to investigate at which limit that the particle could be subjected to processing. This study attempted to predict particle breakage using mechanical test with image analysis as method validation. The characterization of different coarse particles was done using the developed methods on mechanical tests and image analysis. The mechanical tests involved double compression (texture profile analysis), that can measure hardness, maximum stress, modulus, springiness, cohesiveness, and chewiness. Single compression and puncture tests measured bio-yield stress. Results show that the tests gave different trends of particle strength. Representative particles were run on the designed rig composed of three-unit operations: agitator, wing rotor pump and restriction pipe. Morphological changes were measured by image analysis indicating the breakage due to the unit operations. The results of image analysis cannot be correlated to the mechanical properties because not all particles did significantly break. For rapid measurement of particle breakage, sieving analysis is recommended on obtaining particle size distribution. Nevertheless, image analysis complements to this method as it can still provide shape parameter information that is also helpful on understanding mechanism of particle breakage.

Keywords: Particle breakage, Mechanical test, Image analysis, Unit Operation, Bio-yield test

Executive Summary

The global economy is increasingly competitive. Consumers generally pay attention to the safety and conformity aspects of the food products that they buy and consume, but their potential expectations with respect to quality involves different factors. As a food packaging solutions provider, Tetra Pak aims to provide their expertise and knowledge about processing of food products with particles that could maintain the best possible product quality. The knowledge about particle and processing relationship is then vital.

The objectives of the study are:

- To set up parameters for mechanical tests method to measure particle strength that can be used to predict the extent of change in size and shape due to the agitation, passing through wing rotor pump and restriction pipe

- To measure the change in particle size and shape by image analysis method

- To test whether the obtained measured values from mechanical tests and image analysis methods are correlated

- To compare the developed image analysis method with the existing sieving analysis

This study is more into exploring the relationship between particle strength and change in particle morphology due to processing such as agitation, passing through wing rotor pump and restriction pipe.

In this study, the predominant external force considered is axial stress, or vertical stress. There are 4 phases in deformation: elastic phase, bio-yield point, ultimate strength and rupture. Some of the indicators of particle strength are the texture profile parameters and bio-yield stress. Texture profile parameters are maximum stress, modulus, cohesiveness, and chewiness.

These were measured by double compression test, while bio-yield stress was determined using single compression and puncture test, in two probes, 2 mm and 5 mm. These mechanical tests were done using texturometer.

Thirteen samples of fruits and vegetable particles were analyzed for the mechanical properties, and three representative samples, thawed diced carrots, thawed chopped mangoes and canned diced potatoes were subjected to three processing operations. With the set parameters, these are agitation, pumping and

passing through restriction rig. Sample particles were collected, and morphological properties (size and shape) were analyzed. Size was indicated by circular equivalent (CE) diameter, while shape was indicated by circularity, elongation and convexity parameters. These are measured using two apparatus: Digi-Eye for image capturing and Morphologi 4-ID for image analysis.

The study concludes the following:

1. Particle strength can be measured in three different ways. In this study, this property was measured using double compression at the elastic limit and compression and puncture up to the bio-yield point; however, the results have different trend. These results were sought to be correlated to the results of the morphological analysis.

2. Even the pilot scale experiment conditions were intended to be harsher than in the real food processing conditions, the mango and carrot particles did not break significantly based on image analysis. Correlation of the results of mechanical test and image analysis cannot be done because not all the particles tested (2 out of 3) did not significantly break.

3. No conclusion can be derived on the comparison of the three particles tested. Based on the availability of the raw material, thawed mangoes were treated with the different test conditions from the other particles.

4. For more rapid measurement of particle breakage, the existing sieving analysis is still recommended. However, this method is limited to mass and volume-based particle size distribution. For cases that good quality images of particles are desired, image analysis is suggested to be done. Aside from particle size distribution, shape parameters can be obtained that are helpful on understanding mechanism of breakage.

The following are recommendations based on the results and findings of the study:

1. The use of apparatus for mechanical tests that could measure smaller forces is recommended.
2. Apply the same study using other types of particles in order to have more points in the correlation.
3. Other forms of particle breakage like shearing and measurement of stress from fluid can also be examined for correlation studies.
4. For modelling studies, food sample model (e.g. standardized cubic gel particles) could be used in the test instead of using real food sample in order to avoid variation within the sample.
5. In order to investigate the effect of restriction rig, the possible future work that could be done are to provide harsher treatment such as using smaller restriction rig, to increase the fluid flow rate.
6. Perform the same study and focusing on other unit operations. If possible, one-unit operation at a time is recommended to avoid interference of the effects of other operation to the particles.

Acknowledgement

Nuti Hutasingh   Jan Roland Guerrero Molina

Lund, June 2019

Jan Roland Guerrero Molina
Nuti Hutasingh

Table of contents /
Innehållsförteckning

List of acronyms and abbreviations / Akronym- och förkortningslista

CE Diameter	Circular Equivalent Diameter
CN	Canned
FZ	Frozen
TPA	Texture Profile Analysis

List of Figures

xvii

List of Tables

List of Equation

1 Introduction

This section presents the background of the study and highlights the problem description. The purpose and goal are also discussed in this chapter.

1.1 Project Background

1.1.1 General Introduction

The global economy is increasingly competitive. Consumers generally pay attention to the safety and conformity aspects of food products that they buy and consume, but their potential expectations with respect to quality involves different factors. Price, taste, and appearance are some of the immediate properties in assessing food product's quality (Savov & Kouzmanov, 2009). These various aspects of quality make it challenging for the producers to meet the demands of the consumers in the product quality perspective. It is then critical for the producers to perceive and interpret the signals that come from consumers.

One of the most important product quality parameters for consumers is the texture and mouthfeel of the product (Guinard & Mazzucchelli, 1996). These are sensory quality attributes that are perceived by consumers using their mouth, and the preference differ from consumer to consumer. In some cases, this attribute is more important than flavors (Foegeding et al., 2011). Recently, consumers had become even more texture conscious and more appreciative of good texture properties in foods. Due to the growing interest in measuring and understanding consumer attitudes to food texture, extensive research and studies are underway in academia and industry.

The challenge is on the manufacturing to produce food products with the food texture that would be acceptable to their consumers which are usually of wide range of types. With the complexity of consumer demands on food products, product design also becomes more challenging due to the nature of food which is a matrix of different biomolecules. The raw materials, and its combination with other ingredients in the food system, the formulation and the processing these undergo are important technical considerations in the product design. Ultimately, these also affect the sensorial quality of the final product.

1.1.2 Food Particles

Food products with particles in the liquid matrix are growing in the food market. More products are developed with combinations of textures that surprise and delight consumers. Examples of which include yoghurt with pieces of fruit/berries, soups with large pieces of meat, fish and vegetables, ready meals containing beans. Consumers are also choosing products with the right taste and mouthfeel that they desire. It is known that these large food particles suspended in the product influence in the overall texture of the product perceived by customers. In this regard, food particles are given much more attention on product design.

Processing of food particles suspended in liquid medium are be done in many ways and commonly involves many steps. The particles could be exposed to both a harsh mechanical and thermal treatments. Every step affects the quality of the product and could cause changes in texture, colour, shape among quality attributes. In manufacturer's perspective, the manufacture of such products with particles becomes challenging because several unit operations are involved, and there is a target quality of the particles suspended. Typical food processing operation involves pumping, valve passages, heating and cooling, tank storage, and agitation, which are known to have effect on the quality of particles after the processing (Rahardjo, 1992; Rihardio, 1993; Cantu-Lozano et al., 2000). This effect depends on the particle itself, as well as the external thermal and mechanical factors involved in the processing. By using the correct processing equipment and processing parameters, the resulting changes could be mitigated and adapted to the desired properties of a product.

It is an advantage of manufacturers to have a better control of the product quality. By providing this, the company could increase the market value of their products and could reduce the rejection rates and lost orders by customers. In addition to quality control feature, this tool could also give the manufacturers a better understanding of how food particles are affected by the process, and how they could influence the overall change in the particle properties. By characterizing particle quality parameters, production issues could also be understood, and optimize the efficiency of manufacturing processes. This could then increase output or improve yield and stay ahead of the competition.

1.1.3 Tetra Pak

Tetra Pak is one of the world's leading food processing and packaging solutions company. They are known for working closely with their customers and suppliers to provide safe food. The company offers packaging, filling machines and processing for dairy, beverages, cheese, ice-cream and prepared food, including distribution tools like accumulators, cap applicators, conveyors, crate packers, film wrappers, line controllers and straw applicators. Being provider of food processing

2

solutions, their role is also critical in providing the desirable food texture in the final product. Food processing equipment should be properly designed in such a way that the integrity of particles in the matrix are considered to get the target overall texture of the food.

The existing practice in measuring particle quality is sieving technique which is an example of a separation method. The particles are brought on top of a nest of sieves with a sequence of decreasing mesh size, then the particles pass through the compatible apertures. (Merkus, 2009). Though the particle size distribution can be derived from this method, the changes in other characteristics like size and shape cannot be determined. By measuring the morphological properties, the mechanism of breakage of particles due to processing can be understood.

As a food packaging solutions provider, Tetra Pak aims to provide their expertise and knowledge about processing of food products with particles that could still had and maintain the best possible product quality. Tetra Pak tries to understand how unit operations affect the particle integrity in order to provide information of their machine to customers efficiently. At the same time, food producers are aiming for reduced operational costs and increased efficiency in order to be competitive. The knowledge about particle and processing relationship is then vital.

1.2 Research Objectives

Particle characterization is an important tool in ensuring overall texture quality of food products with particles in it. The study involved the development of method that is aimed to deliver the understanding of food particle integrity in the processing systems. The following are the objectives of the study:

- To set up parameters for mechanical tests method to measure particle strength that can be used to predict the extent of change in size and shape due to the agitation, passing through wing rotor pump and restriction pipe

- To measure the change in particle size and shape by image analysis method

- To test whether the obtained measured values from mechanical tests and image analysis methods are correlated

- To compare the developed image analysis method with the existing sieving analysis

This study also aims to investigate the following hypothesis:

The particles with low values obtained from mechanical tests (sensitive particles) will show more change in size and shape during processing, and the less sensitive particles will have less change in size and shape.

The results of the study are expected to be beneficial to food processing equipment designers in the company. The mechanical tests could provide the relevant texture profile and other mechanical properties of particles that can be considered in the design. It could also be used for prediction of the extent of particle breakage at a certain processing condition. Using this tool, the control of quality is already considered even before the fabrication of appropriate processing equipment and manufacturing of food products. Consequently, it could save resources in designing and fabricating equipment that would give the undesired particle quality in the product.

1.3 Scope and Delimitation

This study is more into exploring the relationship between particle strength and change in particle morphology due to processing such as agitation, passing through wing rotor pump and restriction pipe. Two phases are involved – exploring and defining.

In the explore phase, the needs and capabilities are screened, while in the define phase the actual research and development is started in a small scale. The work done in this phase is to provide a "proof-of concept" and the set-up of the experiments are carefully planned. The method is still in a basic mode which is testing one equipment and only few kinds of fruits and vegetable particles. The method is also validated by running in pilot scale run using available equipment like tank, agitator and restriction pipe. The extent of validation though is not thorough because only limited types of particles are involved.

The study involved developing measurement procedures using existing apparatus and methods tailored for the purpose of the study. The particle sensitivity is measured by using texture profile analysis, compression test and puncture test. The assumption is that the predominant mechanism of breakage in the process is axial pressure. Given the available apparatus, the particles involved in this study should have at least one (1) cubic centimeter. Below this dimension, the method on texture profile analysis with the available equipment would not be applicable. In addition, a method on quantifying the change in size and shape are also developed using image analysis. Microparticle properties like charge properties, porosity, and permeability are not considered in this study.

2 Theoretical Framework

This master thesis is based on some concepts, theories and finding from literature and previous research. This chapter guides the reader to go through the relevant reference, thus giving a clear idea about the direction of this paper.

2.1 Particle Deformation

Food particles in liquid medium are subject to different external forces during processing. The liquid medium itself provides shear stress to the particles, and this increases with viscosity (Bouvier, 2011). These particles could interact, by collision to other particles and to the machine walls. Depending on the extent of impact of the collision, the particle integrity is challenged. When the product is in-still condition, say, stored in a package, the large particles could still experience external forces like compression due to gravity. For example, big potato chunks in sauce could settle at the bottom of the package, and this compress the particles at the bottom portion of the package.

In this study, the predominant external force considered is axial stress, or vertical stress. When fruits and vegetable tissues of constant cross section are subjected to compressive loading, they often go through different phases of deformation (Abbott et al., 1997). From Figure 1, during the initial phase of deformation, the force-deformation relationship is relatively linear, and the deformation is elastic. In retrospect, there are several non-destructive or minimally destructive methods had been developed for measuring fruit firmness (Abbott et al., 1997; Gunasekaran, 2001; Lu and Abbott, 2004). As force increases, the force-deformation relationship becomes nonlinear. During this second phase of deformation, only partial recovery could be realized after the release of applied force and cells start to fail but without rupture. The second phase of deformation is culminated with a noticeable drop or no increase in force with increases in deformation. Such a phenomenon is characteristic of many biological materials and is called bio-yield, which is indicative of the failure of cells. Beyond the bio-yield point (third phase), macrostructural failure starts to occur, leading to the final rupture (fourth phase) of the tissue specimen (Lasztity et al., 1992).
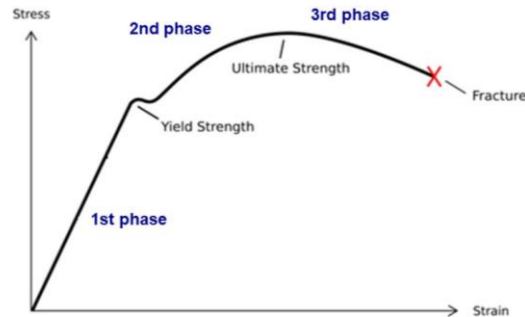
Figure 1 Typical force-deformation curve from compression test of whole fruit (Li, et al., 2017).

2.2 Particle Strength

Several researchers have studied physical properties of various foods. In case of agricultural and food applications, these properties are correlated to mechanical properties, which are then considered for the design of equipment for harvesting, post harvesting technology transporting, storing, cleaning, separating, sizing, packaging and processing it into different food (Li et al., 2017). Without considering the mechanical properties of food materials involved, the resulting designs lead to inadequate applications. Inappropriate designs result in a reduction in work efficiency. Knowing the mechanical properties of food particles would help equipment designers to apply forces properly (Emadi et al., 2009)

2.2.1 Texture Parameters

Since texture is usually based on subjective evaluations, it is important to have objective measurements as well. Several studies had investigated the correlation of objective methods using various apparatus and methods available, and results of sensory evaluation. The difficulty in this kind of correlation is that consumers could have different perceptions of texture. It is important to have calibrated panelists in order to ensure that they had similar language and understanding of the texture. From Table 1, there are several texture parameters that could be used to characterized food materials.

Table 1 Texture parameters that could be measured and calculated from the double compression test (Trinh and Glasgow, 2012).

Texture Parameter (SI unit)	Description
Hardness, N	Force required for a pre-determined deformation
Stress, Pa	Force per unit of area (similar to pressure)
Modulus, Pa	Ratio between the applied stress and the strain produced
Springiness, %	Originally referred to as "elasticity", or the rate at which a deformed sample returns to its size and shape
Cohesiveness, %	Strength of internal bonds in the sample
Chewiness	Energy needed to break a solid food to a specific down size; also referred to as rate of breakdown
Gumminess	Same to chewiness but more related to semi solid food

2.2.2 Bio-yield Stress

Bio-yield stress indicates the noticeable drop or no increase in force with increases in deformation during compression or penetration test. This is also the point at the end of the elastic limit, and where the breakage of the particle starts. Figure 2 shows the deformation curves of canned potato and frozen-thawed carrots.
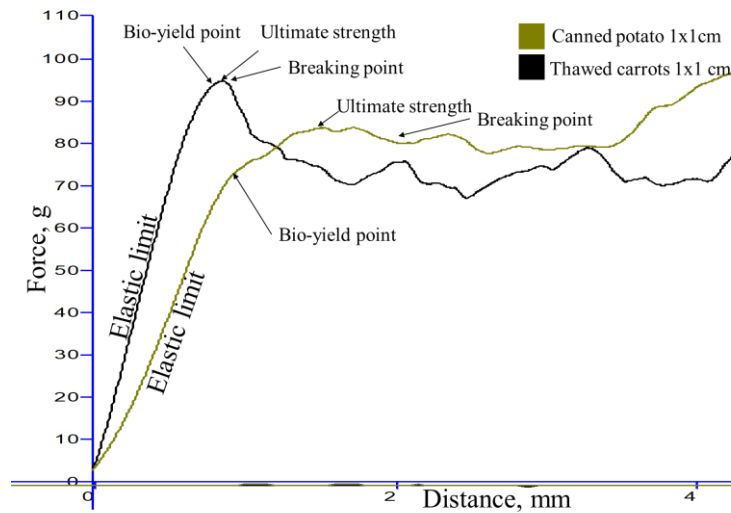
Figure 2 Particle deformation curve of canned potato and thawed carrots particles using 2 mm puncture probe.

7

The concept of using bio-yield force as an indicator of fruit firmness is proposed (Mohsenin, 1986; Lasztity et al., 1992) because it goes beyond the elastic deformation but does not reach the total rupture of fruit specimen. In order to capture this, it must exceed the %strain applied at the elastic limit which is indicated by a linear upward curve in the graph. At the point when the line starts to change slope (no change, or decrease in slope), the bio-yield point is determined. The more % strain applied, the more information about the particle deformation could be gathered. The forces applied during deformation and rupture processes are captured in higher strain.

2.3 Mechanical Tests

Compression test has been widely used to evaluate mechanical behavior of different food products, like bakery, fruits and vegetables. This test has also been used to study deformation rate and degree effects on rheological parameters. This is done by pressing the sample with a cylinder at a known speed, and strain. In this case, the contact area is determined by the surface area of the sample exposed to the cylinder. Preferably, it is suggested to analyze the stress distribution within a food particle by compression and the maximum stresses are determined if it is exceeding the strength of the food particle (Rahardjo and Sastry, 1992).

The phases of deformation of the particle could be visualized by *single compression test* at certain strain that allows rupture of the sample at fixed deformation rate. The applied force (or the stress which is force applied per unit area) during compression is recorded.

One of derivatives of compression test is *texture profile analysis (TPA), or double compression test*. TPA is a common procedure to characterize the texture of vegetables and fruits through extracted mechanical parameters from the force–displacement data of a 2-cycle loading (compression)-unloading(relaxation) of the test probe (Bourne, 2002; Rahman and Al-Farsi, 2005; Tiago et al., 2016). It consists of 4 steps of compression test: compression, relaxation, compression and final relaxation. The behavior in terms of stress of the sample is also recorded through time and/or distance. The amount of time or distance between these compression and relaxation determines several texture profile parameters such as springiness, cohesiveness, gumminess and chewiness, which gives the advantage of this test. The use of this technique had become widespread with the existence of computer assisted texturometers and their softwares for the data analysis. However, it is important to note that the parameters being measured and calculated using TPA should be fully understood because these parameters are not always applicable to all kinds of food. Since TPA parameters vary with sample size and shape, ratio of compressing probe size versus sample, degree of compression,

deformation rate, number of 'bites', and replicates per mean value, all the TPA measurements should clearly state in reports what conditions are used.

The test choice of texture profile analysis depends on the purpose of the test. If the purpose is to imitate the highly destructive process of chewing using teeth, high strain values are required. However, if parameters like springiness and cohesiveness are being sought, then high destructive strain values become meaningless because the second compression cycle does not usually find a weakened sample with just the first internal cracks, but portions or small pieces of the initial sample.

Several authors had modified some of these texture parameters. Trinh and Glasgow (2012) presented the issues related to the definitions of the TPA parameters and important considerations for the test operating conditions. The typical graph of TPA is shown is Figure 3.

Figure 3 Typical force – time curve of double compression of an elastic particle.

Source: https://texturetechnologies.com/resources/texture-profile-analysis#tpa-measurements

The graph is time or distance travelled by the probe versus the force 'felt' by the probe from the particle. The trigger force is set, and this is the force wherein the probe will start measuring. Point 1 to Point 2 indicates the initial compression, Point 2 to Point 3 is the relaxation while the probe is still in contact with the sample. Point 3 to Point 4 is the lag time when the probe stops and could allow the particle to recover from deformation, if any. For test that had no set lag time before the second compression, this gap means the distance of deformation, or sometimes there is no gap if the particle is elastic. Points 4 to 6 indicates the second compression and relaxation.

The use of *puncture test* is done in order to measure the maximum force or firmness of different food products. This is usually applied to different cultivars of

fruits and vegetables (Chen & Rosenthal, 2015). Usually, a penetrometer which could be handheld is used for the measurement (Lu, 2005). The procedure is the same as in compression test, however they differ on the probe being used. In puncture test, the contact area of the probe and the sample depends on the probe size because the surface area of the sample is higher than the probe. There are several types of puncture probes available, and the application differs from the objective of the study.

2.4 Particle Morphology

The behavior and texture of food particles are dominated by its physical properties, in addition to its biochemical properties. For large and coarse particles, these physical properties could also be indication of its overall texture and mouth feel of the final product. From a manufacturing and development perspective, some of the most important physical properties to measure are particle size, particle shape, mechanical properties, surface properties, charge properties, and microstructure. However, not all these mentioned properties are applicable to all ranges of particle sizes. For example, surface charge properties and microstructures could be more relevant to very minute particles in the case of emulsions and foams. Depending on the material of interest, some or all of these could be important, and they may even be interrelated, like surface area and particle size. The most significant and easy to measure properties are usually particle size and particle shape.

2.4.1 Particle Size

One of the ways to measure particle size is considering the distance from point to point in the particle. This would tell how big or small the particle is. Table 2 shows classification of particles in terms of fineness, according to Merkus (2009).

Table 2 Classification of particles according to size range (Merkus, 2009).

Fineness	Size Range
Nanoparticles	$< 0.1 \mu m$
Ultrafine	$0.1 - 1 \mu m$
Fine	$1 - 10 \mu m$
Medium	$10 - 1000 \mu m$
Coarse	$1 - 10$ mm
Very coarse	> 10 mm

In this study, very coarse particles are involved. From Figure 4, examples of which are cubes of potatoes and carrots, whole blueberries, cross sectional cut olives, among others.

Being a three (3) dimensional material, the basic dimensions of a particle are the following: length, width, height, surface area, volume, and diameter (see Figure 4). Food particles that are large could be directly measured manually using appropriate apparatus like ruler or caliper. Other size parameters like volume and surface area could be calculated based on the empirical measurements obtained.
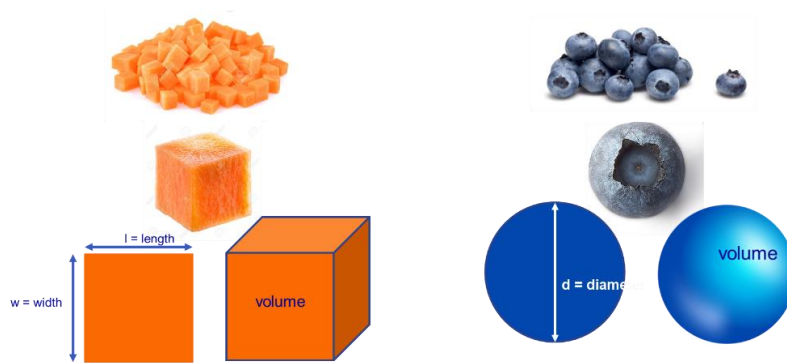
Figure 4 Dimensions of simple and basic shapes (cube and sphere) of food particles.

For it to be easier to analyze particles, ideally, it is assumed that particles had uniform size and shape. However, particles suspended in food matrix are not uniform which makes the measurement complicated. They have different particle sizes (see Figure 5), different forms which could be regular or irregular or even different particle shape. Due to its heterogeneity, it is important to consider all the sizes of particles in the matrix. Usually there is the normal or target particle size which dominates in the food system in terms of number frequency, or in terms of volume. This variation in size could be reflected in *particle size distribution* that is usually used in very small particles, and it could also be applied to larger and coarse particles.
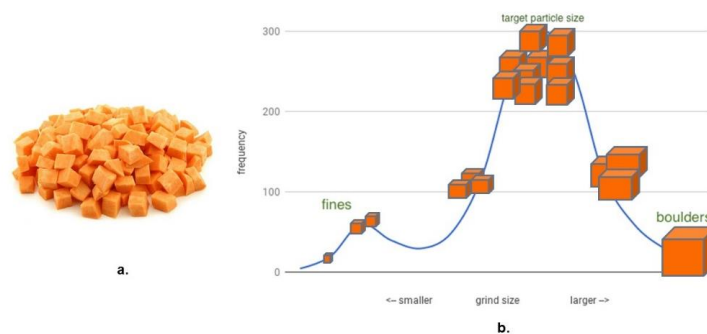
Figure 5 Sample particles, in the case of cubed carrots (a.); Example of particle size distribution (b.).

Merkus (2009) also classified the width of the particle size distribution accordingly (see Table 3). When the particles in the sample had completely uniform size, it could be considered as mono-sized particle food system, and the ratio of the cumulative undersize particle size of 90% of number of particles, and the size of the 10% is equal to 1. On the other extreme, a food system had a very broad range of particle size if the ratio is more than 10. In this case, there is no 'normal' particle size in the system because the sizes are very heterogeneous.

Table 3 Nomenclature on width of particle size distribution (Merkus, 2009).

PSD width	D_{90} / D_{10}
Mono sized	< 1.02 (ideally 1.00)
Ultra narrow	1.02 – 1.05
Narrow	1.05 – 1.50
Medium	1.5 – 4.0
Broad	4.0 – 10
Very broad	> 10

One of the complexities in particle size measurements is that actual particles do not have the same dimensions. Most particles are not spherical nor cubic and had different shapes and often rough surfaces and in numerous frequencies in the food system. It would be tedious to measure each of the particles manually. In small particles, image analysis or light scattering techniques is done in order to determine the sizes of particles, and the frequencies of these sizes in the sample. Light scattering technique involves sophisticated analytical system in order to measure particle sizes, and this is not yet done in very big particles because it would be more impractical. On the other hand, image analysis is more straightforward because it will only involve good image capturing, and image analysis. However, the limitation of this technique is that the measurement of the size is from the 2-dimensional form of the particle. The image is obtained by just 'reading' the top view image of the particle as its 2D form (Figure 6).
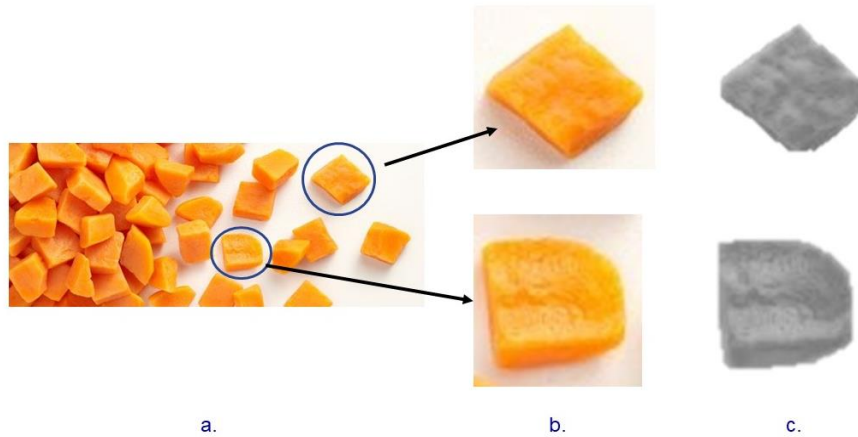
Figure 6 Conversion of particle images into their 2D form.

Particles are 3-dimensional objects, and unless they are perfect spheres like emulsions or bubbles, they cannot be fully described by a single dimension such as a radius or diameter. In order to simplify the measurement process, it is often convenient to define the particle size using the concept of equivalent spheres. In this case, the particle size is defined by the diameter of an equivalent sphere having the same property as the actual particle such as volume or mass for example. It is important to realize that different measurement techniques use different equivalent sphere models and therefore will not necessarily give the same result for the particle diameter. In several studies (Wadell ,193; Wadell, 1933; Johansson & Vall ,2011), and from manual guides of suppliers of particle size analyzers, the area of the 2D image of the particle is converted first into its circular equivalent (CE). With the 2D image and its CE having the same area, the diameter of the circle (CE diameter) could be calculated. This CE diameter could also be used to calculate for the volume of the particle's sphere equivalent (SE) (see Figure 7).
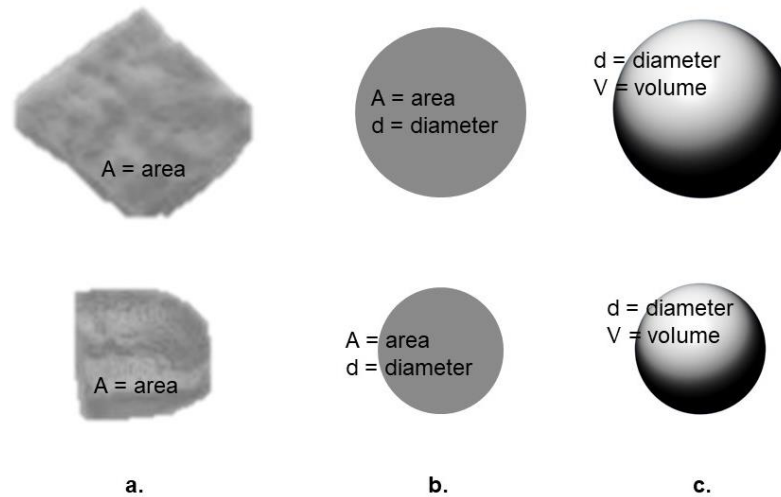
Figure 7 Two dimensional image of the particle (a.); Circular equivalent (CE) of the particle (b.); and Sphere equivalent (SE) of the particle (c.).

The equivalent sphere concept works well for regular shaped particles. However, it may not always be appropriate for irregular shaped particles, such as long rods and cylinders, where the size in at least one dimension could differ significantly from that of the other dimensions. It is still then important to consider other particle characteristics.

The particle size parameters give the idea on how big or small the particles are, and the variety of particle sizes in the given food system which might had effect on the texture quality of food.

2.4.2 Particle Shape

The other relevant particle characteristics that is considered is the *particle shape, and these could be described qualitatively and quantitatively*. As mentioned, particles suspended in food matrix are not in uniform size and form. They could have a wide variety of shapes and forms, from cubic, spheres, cylinders, rectangular prism and other irregular shapes. In this case, it is challenging to quantify these various shapes especially if they are not regular. The overall form of the particle could be measured by simple measurement on aspect ratio, or the ratio of the width and length of the particle. The value for symmetrical particles is getting close to 1, while asymmetrical shapes had low values.

14
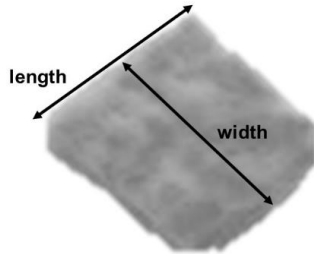
Figure 8 Considerations in aspect ratio or elongation.

According to (Mora & Kwan 2000) there are three (3) universal shape parameters that are considered: elongation, circularity, and convexity. In order to quantify the shape of the particles, some of the particle size parameters are also considered.

Elongation value equates to the ratio of the length of the minor axis (width) with the major axis (length). This is the reciprocal of aspect ratio (Figure 8). A rod, for example, had a high Elongation value, while perfect circle and square which had equidistant axes had elongation value equal to zero.

Circularity could be measured in different ways, and these are presented by Riley (1941), Hawkins, (1993) and Rodriguez, (2013). In this study, circularity is considered as the ratio of the circumference of a circle equal to the object's projected area to the perimeter of the object (see Figure 9). A perfect circle had circularity of 1.0, while a very narrow elongated object had a circularity close to 0. (see Table 4)
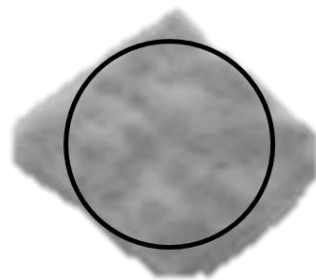
Figure 9 Illustration of circularity of a particle.

Convexity is the perimeter of the convex hull perimeter of the object (circumscribed boundary) divided by its perimeter (see Figure 10). Convexity is a measure of how 'spiky' a particle is.

15
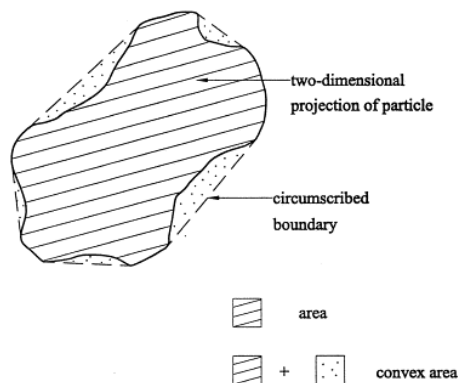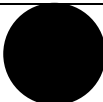
Figure 10 Parameters in determining convexity of particle (Mora and Kuan, 2000).

The convex hull could be the border created by an imaginary rubber band wrapped around the object. In the diagram below B is the added 'convexity area' of the particle surrounded by the convex hull. The Convexity values are in the range 0 (least convex) to 1 (most convex)

Size and shape are some of the physical properties that are important to characterize large particles. These properties are the ones particles had on a certain instance, say, before or after it undergoes processing. The values could change, and the extent of change could vary depending on the biochemical properties of the particles as well as the external forces acting on them.

Table 4 Values of shape parameters of different shapes. (Morphologi 4-ID user manual, 2018).

Shape	Circularity	Convexity	Elongation
	1	1	0
	0.64	0.96	0.82
	0.89	1	0
	0.67	1	0.79
	0.50	0.59	0.24
	0.35	0.69	0.83

16

3 Materials and Methods

In this chapter, the materials and equipment used, and the methods on carrying out the tests and experiments are described.

3.1 Sample Materials

In this study, several different food particles were used. They also came in different formats – frozen, chilled, and canned, and in different dimensions. The particles are commercially available, and the specific variety of these fruits and vegetables are not determined. Table 5 presents the particles involved in the study.

Table 5 List of sample particles analyzed for mechanical properties.

Particle	Brand	Format	Dimensions, cm	Assigned name
Potato	Felix	Frozen	1x1	Potato FZ
Potato	Skalmans	Chilled	1x1	Potato CH
Potato	Vatternpotatis	Canned	1x1	Potato CN
Carrots	3N Produckter	Frozen	1x1	Carrots FZ
Carrots	Noliko	Canned	1x1	Carrots CN
Blueberry	Polarica	Frozen	whole	Blueberry FZ
Raspberry	Polarica	Frozen	whole	Raspberry FZ
Strawberry	Magnihill	Frozen	whole	Strawberry FZ
Mango	Polarica	Frozen	2x2	Mango FZ
Mango	Magnihill	Frozen	1x1	Mango 1x1 FZ
Mango		Chilled	1x1	Mango 1x1 CH
Peach	Sun Valley	Canned	halves	Peach CN
Olives	Pedros	Canned	Slices	Olives CN

3.2 Measurement of Particle Strength

3.2.1 Sample Preparation

The sample particles were in different format like frozen, chilled or canned in-medium. Approximately 100 grams of frozen and chilled particles that are not in any suspending medium were dispersed on a tray for proper thawing, until it reaches the standard temperature of 20ºC (Figure 11). Likewise, approximately 100 grams of particles suspended in medium were washed and drained until the particles of interest had no adhering medium. These particles should also have temperature of 20ºC. It is important to handle the particles gently before doing the tests.

Figure 11 Thawing of carrots.

3.2.2 Contact Area and Particle Orientation

The contact area is important in compression test in order to consider the stress, or the force applied per unit area. Without considering the particle dimension for compression test, the stress and strain value could not be made (Singh and Reddy, 2006; Aviara *et al.,* 2007). For compression test, the contact area is the area of the particle wherein the force is applied, while for penetration test, the contact area is equal to the size of the probe. The usual particle geometries are cube (diced potato and carrots), sphere (blueberry), rectangular prism (chopped bell peppers, potato, carrots), cylinder, and irregular shapes. It is important to consider though that the standard size of the particles should be at least close to 1 cm^3. Ten (10) pieces of the particles were measurements to consider the variations in the sample.

The contact areas of geometries with having constant contact area during compressions such as in cube, rectangular prism, and cylinder were calculated (see Table 6). The relevant dimensions like width, length and height were measured manually with caliper (see Figure 12).
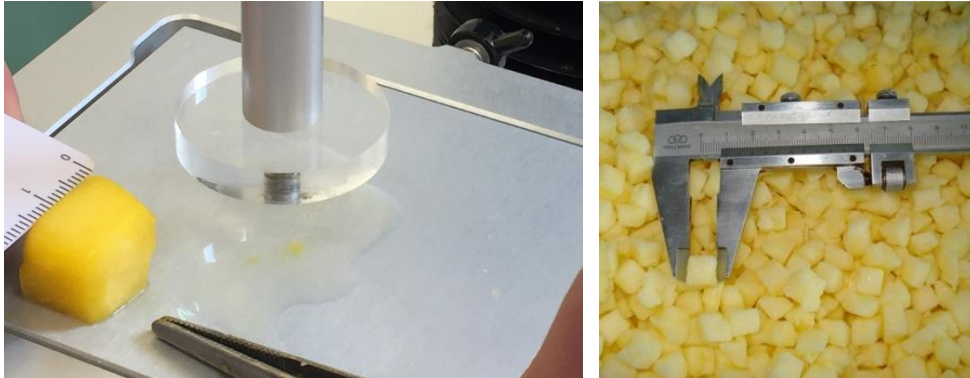
Figure 12 Measurement of dimensions of regular shaped particles (mango and potato) using ruler or caliper.

However, the measurements for geometries with changing contact area through time, such as in spheres and irregular shapes are more complicated and the measurement of contact area had different considerations (see Table 6). From Figure 13, a transparent cylinder with approximately 1 cm height was used to compress the particle up to 10% strain, and the circular contact area could be seen. The diameter of this circle was manually measured using caliper, and the contact area was estimated.
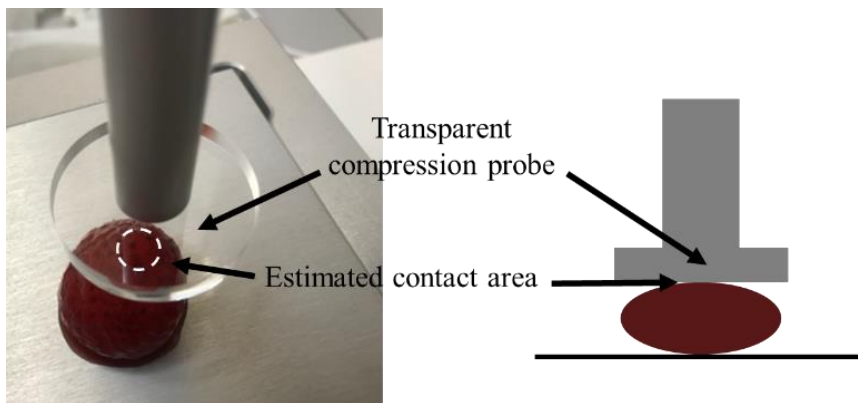
Figure 13 Estimation of contact area for strawberry.

Table 6 Important considerations in the different geometry of particles measured.

Geometry	Examples	Characteristics in compression	Important dimensions measured	Formula for contact area	Orientation during compression
Cube	Diced potato, diced carrots	Constant area during compression	Side (S)	S^2	Does not matter
Sphere	Blueberry	Changing constant area during compression	Radius (r) or diameter (D)	πr^2 or $\pi(D/2)^2$	Does not matter
Rectangular prism	Chopped potato, chopped carrots	Constant area during compression	Width (w) and length (l)	(w) x (l)	Should be consistent across all
Cylinder	Crosswise chopped carrots	Constant area during compression	Radius (r) or diameter (D)	πr^2 or $\pi(D/2)^2$	Circular base
Irregular	Strawberry, raspberry	Changing constant area during compression	Radius (r) or diameter (D)	πr^2 or $\pi(D/2)^2$	Apex up
Particle with skin	Chopped tomato, bell pepper	Constant area during compression (cubic or rectangular prism form)	Width (w) and length (l)	(w) x (l)	Skin down

The assumption on the regular geometries is that they are in perfect form, and they did not have uneven sides. With these assumptions are the limitations of the measurements. Particles are not in perfect and in uniform shapes, making the measured dimensions as estimates of the actual. This is the same scenario with the particles with changing contact area through time. However, at this point, this

could be the best estimates of the contact area of the particles. In addition to contact area, the particle height is also required by the Exponent software, and this could also be measured manually using a caliper, from the base where the particle is laid down up to the tip of the particle.

3.2.3 Mechanical Test

The particles were characterized according to their mechanical properties such as texture profile which is measured at the elastic limit of the particle and the bio-yield stress. The tests were done using TA.XT2 model of texturometer by Stable Micro Systems Ltd. Figure 14 shows the typical parts of texturometer. Exponent software was used for the data gathering and analysis. There were three (3) cylindrical probe sizes used in the particle mechanical tests (see Figure 15).
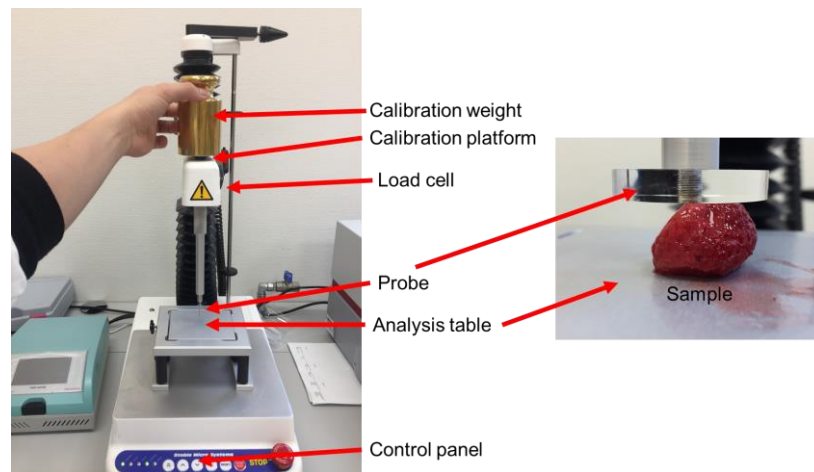
Figure 14 Parts of the texturometer.

Figure 15 Probes used in mechanical tests – puncture probes (2 mm, left) and (5 mm, center), compression probe (36 mm cylinder).

Source: https://www.stablemicrosystems.com/Probes.html

3.2.3.1 Calibration Procedure

Before doing any of the tests, the apparatus should be calibrated. From the tool bar menu of the Exponent software, 'T.A.' tab is clicked, then 'Calibrate', and 'Calibrate Force'. It is important that the texture analyzer's table and loadcell are free from any material. The installed loadcell capacity is also identified – in this case, the apparatus has 5 kg loadcell capacity, and the calibration weight is 2000 grams (g). A window showing that the calibration is complete should be displayed before removing the weight from the calibration platform.

The probe height is also required to be calibrated when measuring parameters in % strain, recording the height of the product during the test, using a button trigger, and starting each test from the same position. From the tool bar menu of the Exponent software, 'T.A.' tab is clicked, then 'Calibrate', and 'Calibrate Height'. It is also important that during calibration, the texturometer table is clear from any sample, and the position of the probe should be as close to the base. The return distance and speed was set to 100 cm and 5 mm/sec respectively. A window showing that the calibration is successful should be displayed.

3.2.3.2 Double Compression Test (Texture Profile Analysis)

The texture profile of the particles was determined at their elastic limit. This is the range of force as to which the particle does not exhibit permanent deformation (Li, Miao & Andrews, 2017). However, this applicable strain at this portion of the deformation curve varies from particle to particle. In this method, a universal test parameter setting was sought for appropriate comparisons among particles. Preliminary tests were done on setting up the test parameters for mechanical test and are presented in Appendix G. The %strain chosen was enough to measure small deformations on firm particles, but not so high to break very soft particles.

The force and probe height of texture analyzer are calibrated before performing any test.

In the Exponent software, the texture analysis setting, or "T.A. settings" is set (see Figure 16). There are default settings in the "Library" when this tool is clicked, then choose "Cycle until Count".

Caption	Value	Units
Test Mode	Compression	
Pre-Test Speed	1,00	mm/sec
Test Speed	1,00	mm/sec
Post-Test Speed	2,00	mm/sec
Target Mode	Strain	
Strain	20,0	%
Count	2	
Trigger Type	Auto (Force)	
Trigger Force	2	g
Advanced Options	Off	

Figure 16 Setting of test parameter for double compression test (texture profile analysis).

The test parameters of the double compression (texture profile analysis) is shown in Table 7.

Table 7 Test parameters of double compression test (texture profile analysis) at different %strains.

Test setting parameters	%Strain	
	10%	**20%**
Probe type	36 mm cylinder probe	36 mm cylinder probe
Number of cycles	2	2
Pre-test speed, mm/s	1.0	1.0
Test speed, mm/s	0.50	1.0
Post-test speed, mm/s	1.0	2.0
Trigger force, g	2.0	2.0

The strain applied is in terms of percentage (%) of the height so that it would be applicable to all particles. After obtaining the graph from the double compression test, the texture profiles were determined by running the macro file which is a method of automating the analysis of a curve. It is a program that could allow to do many complex tasks with just a single action. In this case, a set macro named 'Simplified TPA' which contains the basic calculations for TPA parameters was used. There is also a separate macro file to determine the modulus of the curve. The commands in the macro are based on the formulas of the parameters shown in Table 8.

Table 8 Relevant TPA parameters measured in the particles.

Texture Parameter (SI unit)	Description	Formula
Hardness, N or g	Force required for a pre-determined deformation	Peak at the first point (see Figure 3)
Maximum stress, Pa	Force per unit of area (similar to pressure)	$\dfrac{\text{Hardness}}{\text{Contact area}}$
Modulus, Pa	Ratio between the applied stress and the strain produced	$\dfrac{\text{change in stress}}{\text{change in strain}}$
Springiness	Originally referred to as "elasticity", or the rate at which a deformed sample returns to its size and shape	$\dfrac{\text{Distance 2}}{\text{Distance 1}}$ see Figure 3.
Cohesiveness	Strength of internal bonds in the sample	$\dfrac{\text{Area 2}}{\text{Area 1}}$ see Figure 3.
Corrected chewiness	Energy needed to break a solid food to a specific downsize; also referred to as rate of breakdown	Maximum stress*Cohesiveness *Springiness

It should be emphasized that the chewiness parameter was modified by using the maximum stress instead of hardness. This is to normalize the use of 'firmness' attribute across all types of particles for whatever contact area involved.

3.2.3.3 Single Compression and Puncture Tests

The single compression test and puncture test involves only one round of compression, until it reaches the set %strain at the set probe speed. The difference between these two tests is that, the single compression uses 36 mm cylinder probe, and the measurement of particle contact area and height discussed earlier is important because the probe surface is larger than the particle surface. On the other hand, puncture test does not need the surface area of the particle because of the probe contact is smaller anyway. Two (2) puncture probe sizes were used – 2 mm and 5 mm, as shown in Figure 15. These are standard probes available that are less than the particle size dimensions. The contact area for the 2 mm probe is 3.14 mm^2, while 19.16 mm^2, and these are calculated using the formula below:

Equation 1   **Contact area of the probe** $A = \pi r^2$

where r is the radius in mm

In the Exponent software, the texture analysis setting, or "T.A. settings" is set (see Figure 17). There are default settings in the "Library" when this tool is clicked, then choose "Return to Start".

Caption	Value	Units
Test Mode	Compression	
Pre-Test Speed	1,00	mm/sec
Test Speed	1,00	mm/sec
Post-Test Speed	10,00	mm/sec
Target Mode	Strain	
Strain	70,0	%
Trigger Type	Auto (Force)	
Trigger Force	2	g
Advanced Options	Off	

Figure 17 Setting of test parameter for single compression and puncture tests.

These tests are both tests to determine the bio-yield stress of the particle. This value indicates the noticeable drop or no increase in force with increases in deformation. This is also the point at the end of the elastic limit, and where the breakage of the particle starts (see Figure 2).

The food material used in test run are 1 cm^3 canned potato cubes (Vatternpotatois, Sweden), 1 cm^3 frozen carrot cubes (3N Produckter, Sweden) and approximately 2 cm^3 frozen mango cube (Polarica, Peru). The selected three different sample are based on their difference in sensitivity based on the results of mechanical tests. This is to ensure that the degree of breakage will be different among samples. In addition, the availability of sample, cost efficiency, and regularity of sample are also considered in the selection of representative sample particles.

3.3 Pilot Scale Experiment

A mock processing was done in order to challenge the particle strength by passing through a restriction pipe. Agitator was used to disperse the particles into the suspending medium, and wing rotor pump was used to run the particle mixture into the pipe up to the disposal tank. The setup of this processing is shown in Figure 18.
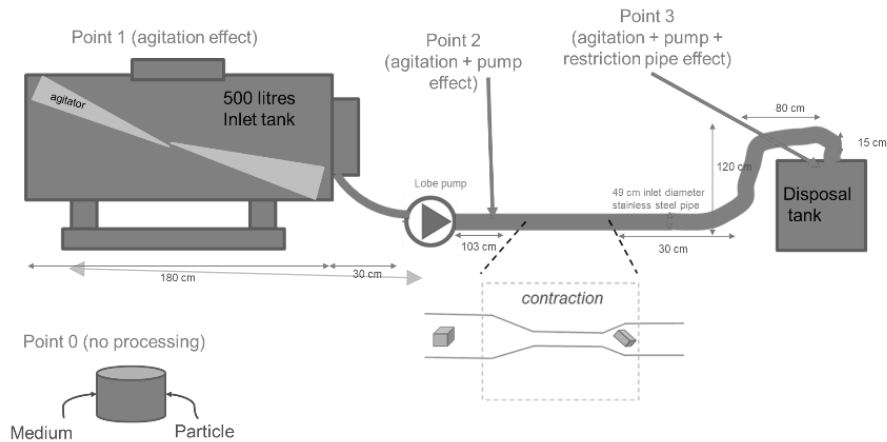
Figure 18 Experimental set up of the processing, and the critical sampling points.

Preliminary experiments were done in order to set the desired set up for the pilot scale experiment aiming to have measurable breakage of the particles. The details of which are shown in Appendix H. The final settings of the experiment are shown in Table 9.

Table 9 Settings of the experiment.

Parameter	Values
Suspending medium composition	2% CMC CEKOL 700 (w/w) in water 4 kg + 200 kg water
Suspending medium viscosity	200 mPa.s
Particle concentration (w/w)	23% (60 kg particle + 204 kg suspending medium)
Agitator tip speed	0.47 m.s^{-1}
Target flow rate	3 m^3.h^{-1}
Actual flow rate (average)	2.77 m^3.h^{-1}
Type of pump	Wing rotor pump
Pump frequency	10 Hz
Restriction pipe	16 mm – for carrots and potato (approx. 1cm^2) 26 mm – for mango (approx. 1.7cm^2)

A known amount of the representative test particles was carefully added into the suspending medium in a 500-liter capacity (inner length of 1.8 meters) 2-blade agitator with scraper (see Figure 19a), and mixed for 45 seconds. While agitator is turned on and by using a wing rotor pump (see Figure 19b), the mixture is pumped through the restriction pipe (see Figure 19c), up to a 1000-liter reservoir tank. As soon as the pump was turned on, 2 kg of particle in CMC medium are periodically collected every 30 seconds at the point after the restriction pipe. After getting samples at Point 3, the operation is stopped in order to get samples at Point 1 and Point 2. The samples were stored in the chiller (4ºC) for 15 hours.
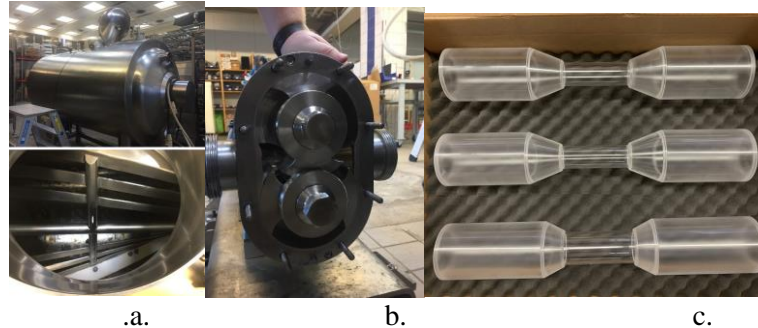
Figure 19 Tank with agitator (a); wing rotor pump (b); restriction pipes (c).

The comparisons of the following samples from different sampling points were done in order to determine the effect of each of the unit operations to the size and shape of the particles:

Point 0 and Point 1 to determine the effect of <u>agitation</u>

Point 1 and Point 2 to determine the effect of the <u>wing rotor pump</u>

Point 2 and Point 3 to determine the effect of the <u>restriction pipe</u>

Point 0 and Point 3, to determine the effect of <u>over-all processing</u>

3.4 Measurement of Particle Morphology

3.4.1 Sample Preparation

The particles were gently stirred in the container to get a well dispersed particles. These were poured into sieve with 2 mm mesh size, and were washed with lukewarm water (approximately 40°C) in order to remove the adhering suspending medium. To drain, the sieve was tilted approximately 20°C for 2 minutes (see Figure 20). The washed and drained particles were then placed on a clean plastic container.

Tilt 17-20° from the horizontal

Figure 20 Draining of particles.

3.4.2 Sample Dispersion

A standard black colored frame (21.0 x 28.5 cm) was used where the particles were dispersed. One hundred (100) grams of potato particles were placed into the frame; 75 g carrot particles and 150 g for the mango particles.

Particles were gently dispersed into the appropriate frame board using spatula or small plastic fork (see Figure 21). The particles were carefully dispersed into the frame in such a way that particles do not attach to each other (approximately 1-2 cm. space), and not too close to the edge of the frame. The labels were appropriately labeled.

Figure 21 Dispersion of the sample using small forks.

3.4.3 Image Capturing

Digi-Eye – DigiPix System S/N DE00296 is the instrument used to capture high quality image of samples (see Figure 22). It provides good and uniform lighting when taking images. This is important in making sure that the samples receive the same levels of illumination and shadowing, and the details of the particle outline were captured properly.

Figure 22 Digi Eye – the apparatus used in capturing images of the particles.

Every time before performing image capturing, calibration of the apparatus was done. This is done by selecting the 'Calibration wizard' on the tools bar. White and colored boards are used in the calibration. The steps indicated in the software were followed.

Figure 23 Frame inside the Digi-Eye apparatus.

The imaging frame with its handle facing to the door of the Digi-Eye was placed to the apparatus guided by the markers (see Figure 23). The markers ensure that the taken picture will include all the particle. Particle image is captured by selecting the camera sign at tool bar, then choose 'RELEASE' to take photo. It should be saved in the designated folder in **.tif** file. If there are some particles are excluded from the frame or had incomplete image, it is suggested to relocate the particle into a frame and retake the photo.

After obtaining the particle images from the Digi-Eye, cropping the image files was done as the original image contains unnecessary elements that could interfere with the analysis.

The cropping was ensured to be similar among images. Figure 25 shows the area, within the yellow dotted line by which the image should be cropped. The actual length of the frame is around 28.5 cm while the actual width of the frame is 21 cm (see Figure 24). This has corresponding pixel value after the image was cropped properly. It is important to crop the original image to a known actual dimension of the frame in order to determine the accurate pixel-size conversion factor.

Given the existing frame size used and based on the image cropping procedure, the ratio the actual frame size and the corresponding pixel dimensions of the image obtained is 0.0758.

Equation 2
$$\text{Size} - \text{pixel factor} = \frac{\text{Width of the frame, mm}}{\text{Pixel of the width}}$$

The suggested file type for the image analysis is **.tif**.

Width = 21.0 cm.

Length =28.5 cm.

2 cm.
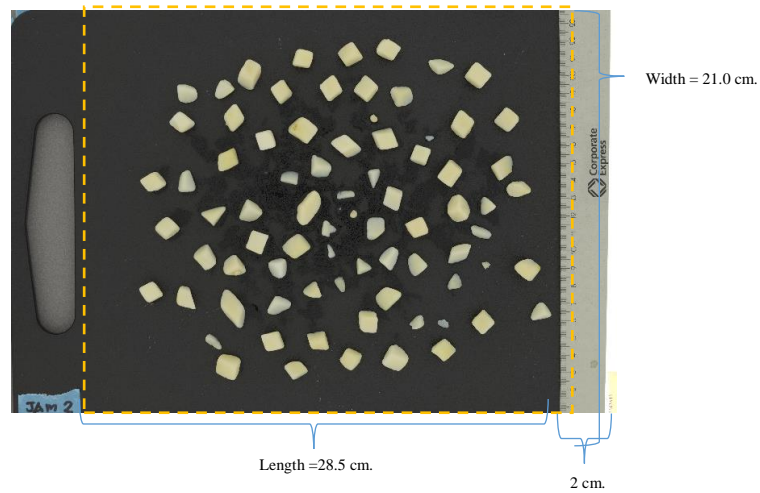
Figure 24 Area of cropping of the image from the Digi-Eye.

3.4.4 **Image Analysis**

The image file generated from the Digi-Eye is then analyzed using the Morphologi 4-ID (Malvern model MOR 2810, 2015) system (see Figure 25). It is an analytical tool that allows to measure and differentiate the morphological characteristics of samples.

Figure 25 Morphologi 4-ID for image analysis.

After obtaining the cropped images with the standard frame dimension (21.0 x 28.5 cm), the images are ready to be analyzed using the software in Morphologi 4-ID. The following are the steps in the image analysis:

1. Open the software and open a new measurement by clicking at the white paper sign at the tools bar.
2. Select 'Measure' at tool bar. Then select 'Image file' to browse the particle picture. If the   instrument does not connect well with the PC, the software will not allow to click at the image file option.
3. Browse the particle images.
4. Input the size of image's pixel (default = 1 μm). It is important to note though that this is not the actual case because of the large particle sizes being analyzed. Too large value for the pixel gives inaccurate readings of the instrument. As mentioned, pixel-size conversion factor is equal to 0.0758.
5. Adjust the particle detection by select 'Foreground Segmentation' at the left-hand side.
6. Select 'Thresholding' as a measurement mode, then adjust the threshold value until the particle is detected well.
7. In some time, choosing 'Estimate' which is the suggested threshold value by the software also   provide good quality particle image.
8. The detected particle should appear in gray scale. If it does appear in blue scale, so click 'Invert'.
9. Click OK, 'Overwrite the SOP' and then click 'START'. Then, the analyzed particle sample will be kept in the 'Records'.
10. The software could analyze the individual type particle characteristics or make comparison among particles.
11. It is also advisable to remove the nuisance 'particles' detected by the instrument, such as very small particles that could be considered as the dust or water droplets. Some particles also attach to each other (see Figure 26) which should be excluded in the analysis to maintain accuracy of the results. For this reason, it is important to properly disperse the particles in such a way that they are not attaching to each other.

Figure 26 Example of attaching particles.

There are several size and shape parameters that could be measured, and different statistical tools that could be used for the analysis. The circular equivalent (CE) diameter is used as size parameter, and circularity, convexity and elongation

parameters are used as quantifiable shape parameters. The details of these are discussed in Chapter 2. It should be noted, though, that the values for the CE diameter reported in the instrument do not take into account the pixel-size conversion, so it is imperative to consider the size-pixel factor discussed previously, which in this case is equal to 0.0758 as calculated during image cropping.

3.5 Sieving Analysis

The sample preparation for sieving analysis is also the same as in morphology analysis. The particles should be washed and drained properly. The particles analyzed were the samples collected from P0 and P3 with 4-minute agitation.

Tables 10 and 11 shows the sets of sieves are used in the sieving analysis of the particles:

Table 10 Set of sieve (Endecotts Ltd., London) used in sieving analysis of carrots and potato particles (1cm^2).

Description	Mesh Standard US	Sieve size, μm	Sieve size, mm
Sieve ASTM Mesh	5/16	8000	8.00
Sieve ASTM Mesh	3,5	5600	5.60
Sieve ASTM Mesh	7	2800	2.80
Sieve ASTM Mesh	18	1000	1.00

Table 11 Set of sieve (Rudolph Grave AB) used in sieving analysis of mango particles (1.7cm^2).

Description	Mesh Standard US	Sieve size, μm	Sieve size, mm
Sieve ASTM Mesh	7/16	11300	11.30
Sieve ASTM Mesh	5/16	8000	8.00
Sieve ASTM Mesh	3,5	5600	5.60
Sieve ASTM Mesh	10	2000	2.00

Sieving analysis is carried out by following the steps below:

1. Measure the tare of each sieve and take note of the weights.
2. Build a sieve tower with the biggest mesh (biggest holes) on top and the smallest mesh at the bottom. The sieves must be positioned one over the other so that each sieve can completely collect the particles draining from the sieve above.
3. Weigh 100 g washed and drained particle samples.
4. Pour the sample into the sieve tower and wash out the remaining product from the container using a small portion of water and pour onto the sieve tower.
5. Shake the sample well to get an even distribution of the particles inside.
6. Wash the sieve tower with the sample by pouring 3 x 1-liter water and allow the particles to pass through the sieves. Avoid over-pouring and flooding because it can affect the results when sample leaks out on the sides.
7. Lift the top sieve and allow draining with 45 deg angle with some tissue underneath. Repeat the process for all the sieves.
8. Drain for at least 3 minutes, and blot dry the sieve with tissue, both the outside and inside of the sieve without touching the particles.
9. Weigh each sieve with the drained particles inside.
10. Calculate the ratio of the particles collected from each sieve to the total weight of the particles using the formula below:

Equation 3   Drained weight of particles, g = Weight of the sieve with the particles – Tare weight of the sieve

Equation 4 $$\% \textbf{ Particles} = \frac{(\textbf{Drained weight of the particle collected})}{\sum(\textbf{Draine weight of the particles in each sieve})}$$

11. Graph the data with the sieve size at the x-axis and the %particles on the y-axis.

3.6 Data Analysis

The results of mechanical test from each particle are analyzed if they are significantly different by Analysis of Variance (ANOVA) using multivariate function with Duncan's test at confidence level of 95%.

The comparisons of morphological parameters of particle between before and after each processing unit are analyzed using t-test at confidence level of 95% as mean comparison method.

These were performed by using SPSS statistical analysis software (vers.20).

4 Results and Discussion

This chapter provides the result and discussion derived from the data collected.

4.1 Particle Strength

Different particles were tested for their strengths by application of compression forces. Several parameters were measured based on the applied forces, and calculated values from the graphs derived. It should be noted though that the pre-treatment applied, specific variety, and biochemical structures of the particles were not taken much into account because the goal is only to characterize the available samples presented in Table 5 according to its mechanical properties.

The values of mechanical properties of particles that were used in the pilot scale processing experiment were highlighted in black in the graphs. This is to illustrate their differences on the levels of particle strength.

4.1.1 Double Compression test at the elastic limit

One of the mechanical tests applied to the particle is the double compression, or also called as texture profile analysis. This is done by two rounds of compression-relaxation at the set %strain – in this case, at 10% and 20% strains. Maximum stress, modulus, corrected chewiness and cohesiveness were the texture profile parameters considered.

The maximum stress of the particle is determined as the peak at the first compression of the particle on a stress-displacement graph, and the modulus is calculated as the ratio between the change in stress and the change in % strain. Both of which are parameters for firmness of visco-elastic particles as also used by Trinh and Glasgow (2012) and Li et al. (2017). In the review by Faber et al. (2016), several models for firmness are presented wherein stress and modulus are important considerations. It can be observed that frozen-thawed mango has low levels of maximum stress and modulus. It implies that this particle provide less resistance for the applied strain; thus, considered as softer particles. On the other hand, canned potato particles have high values of maximum stress and modulus,

while frozen-thawed carrot particles have values in the middle of canned potato and frozen-thawed mangoes (see Figures 27 and 28).

A

B
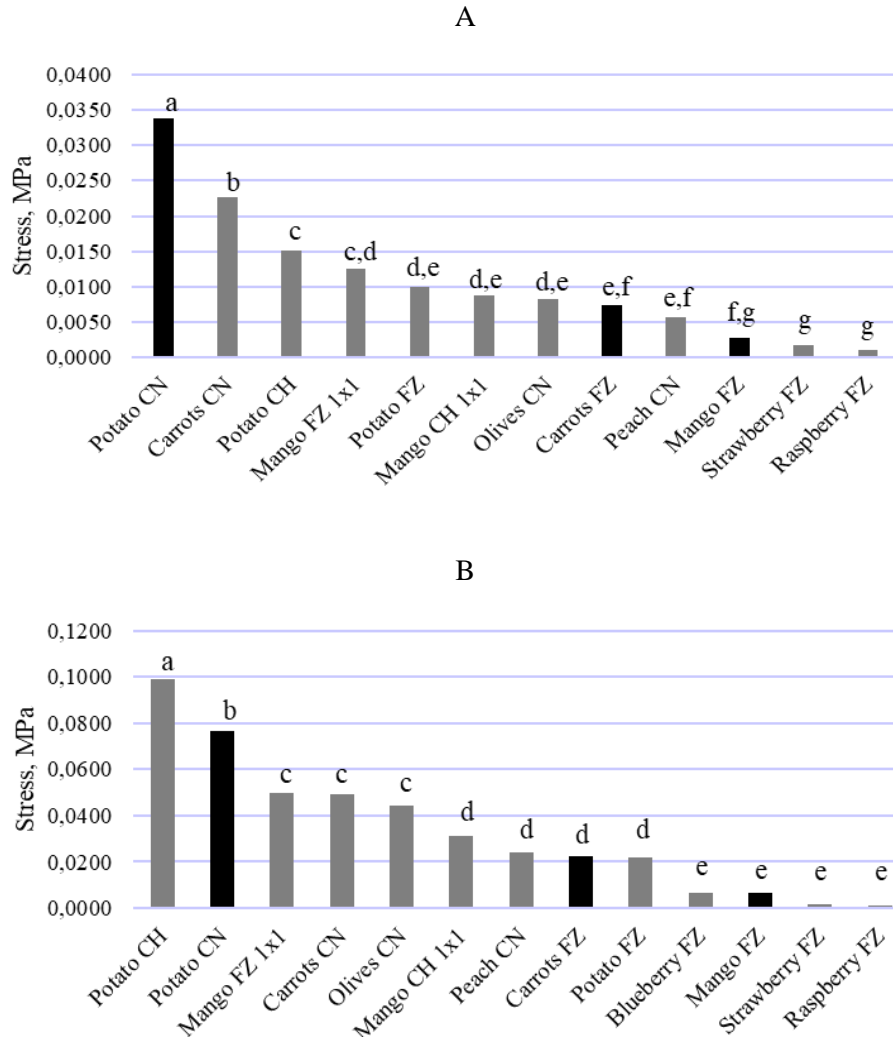
Figure 27 Maximum stress of different coarse particles at 10% strain (A) and 20% strain (B) (Note: Different letters indicate significant difference at 95% confidence level.).

A

B
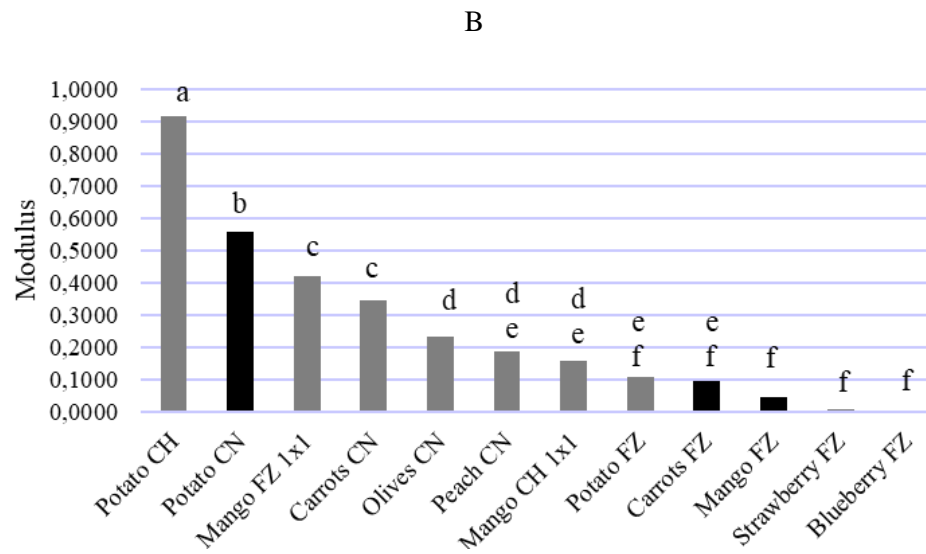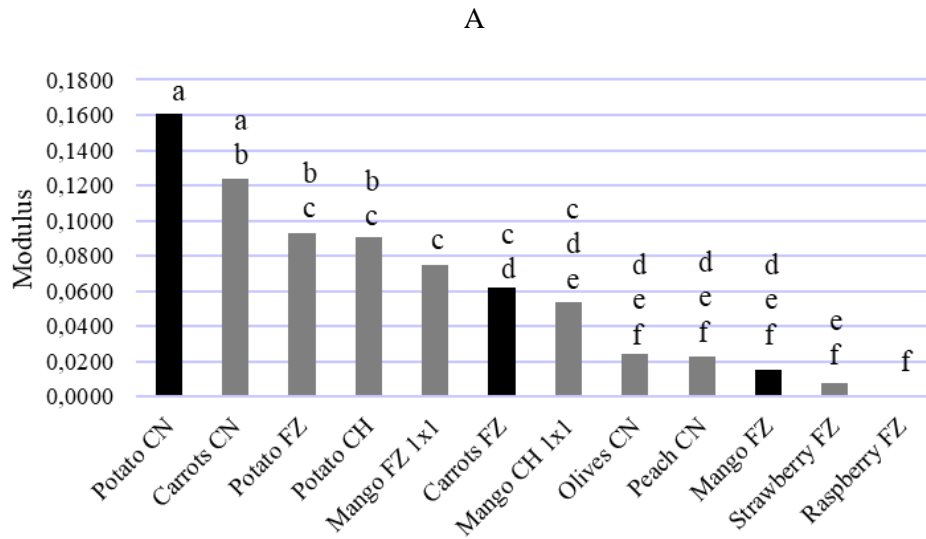
Figure 28 Modulus (in MPa) of different coarse particles at 10% strain (A) and 20% strain (B) (Note: Different letters indicate significant difference at 95% confidence level.).

Cohesiveness (or cohesion) is determined as the ratio of work applied at the second cycle and the work applied at the first cycle (Bourne, 2002; Chandra and Shanasundar, 2015). The work applied (N.m in SI unit) denoted as the product of the force applied (N) and the distance the probe (m) travelled to the particle. Since it was considered that this parameter is measured at the elastic limit, the values should be around 100% denoting that there is no deformation. In this case, the deformation at these low levels of strains applied – 10% and 20% are considered as temporary. The particles are assumed that it can recover from deformation that could take some time. The test parameter applied does not have waiting time after the first compression.

The trend of the values of cohesiveness is different from the trends in the values of maximum stress and modulus of the particles. Frozen-thawed mango, which has low values of 'firmness' parameters, have higher cohesive values than frozen-thawed carrots and canned potatoes, though at 20% strain frozen-thawed mango and carrots are statistically similar (see Figures 29 and 30).
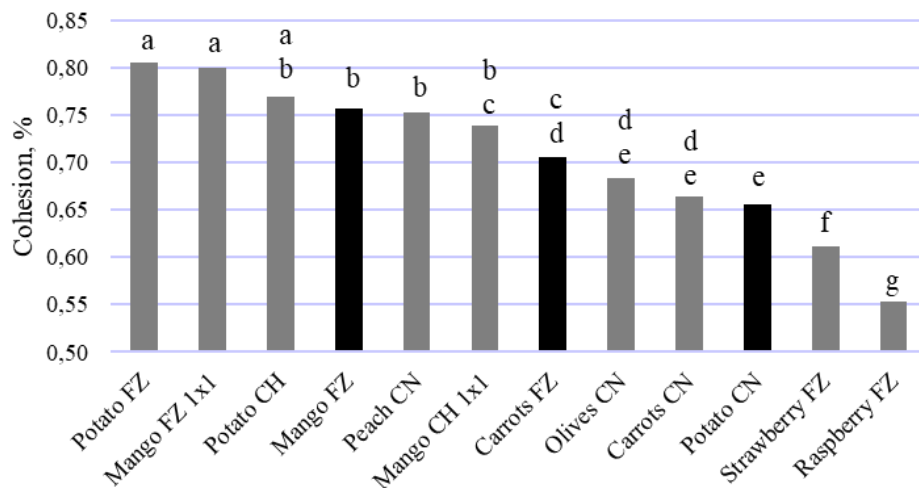
Figure 29 Cohesiveness of different coarse particles at 10% strain.

(Note: Different letters indicate significant difference at 95% confidence level.).
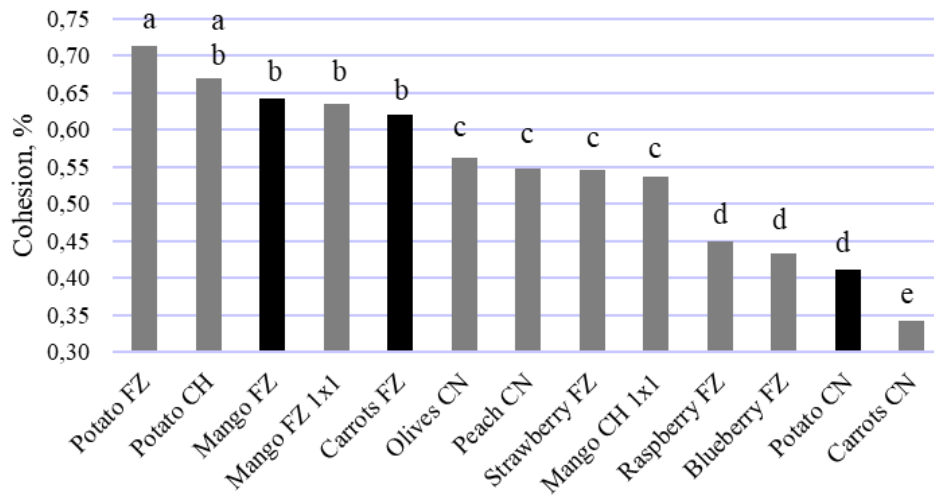
Figure 30 Cohesiveness of different coarse particles at 20% strain

(Note: Different letters indicate significant difference at 95% confidence level.).

Chewiness, in this study considers the maximum stress, cohesiveness and springiness which is the ratio of the distance the probe travelled in the particle at the second compression, and the distance at the first compression. The general trend of the results in this parameter is also similar to the trend of the maximum stress and modulus values. Canned potato, canned carrots, chilled potato and 1x1cm frozen-thawed mango tested have high values of chewiness (see Figures 31).

A

B
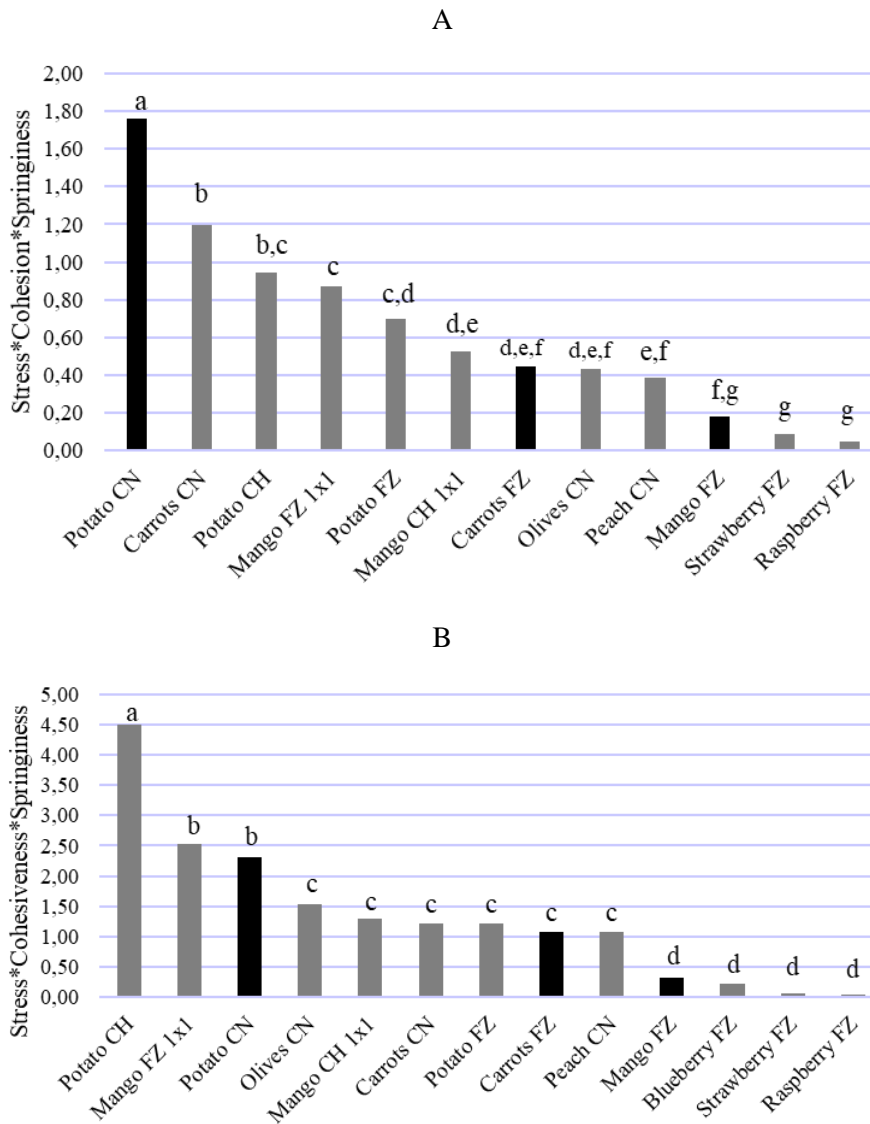
Figure 31 Chewiness of different coarse particles at 10% strain (A) and 20% strain (B) (Note: Different letters indicate significant difference at 95% confidence level.).

As general observations, the particles did not show consistent trend on the stress, modulus and chewiness at 10% and 20%. This inconsistency could be explained by Hertz contact theory that is applicable for small percentage deformations of <10%, and within the elastic limit (Yan et al., 2009). Stress distribution is not uniform when the surface is not very smooth.

4.1.2 Bio-yield tests

Bio-yield stress is the stress when the particles start to break internally. It also indicates the failure of the tissues and cells in the particle. Permanent deformations can occur at this point, and it can initiate the total breakage of the particle when more stress is applied. This parameter was also proposed by Mohsenin (1986) as an indicator of fruit firmness.

This value is determined as the point at the end of the linear regime of the force-time curve of the compression and penetration curves. After the linear regime, there is drop or no increase in force with increase in deformation.

Consistently, frozen-thawed carrot particles have high bio-yield stress values based on single compression and puncture tests using 2 mm and 5 mm probes (see Figures 32, 33 and 34). Frozen-thawed mango has low values of bio-yield stress, and canned potato's bio-yield stress values are in between.
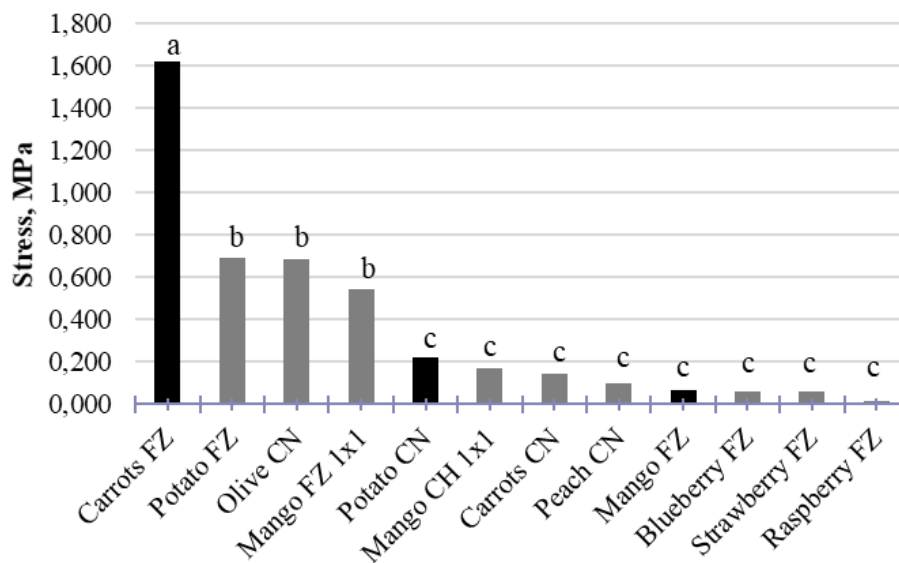
Figure 32 Bio-yield stress of different coarse particles determined by puncture test using 2 mm probe. (Note: Different letters indicate significant difference at 95% confidence level.).
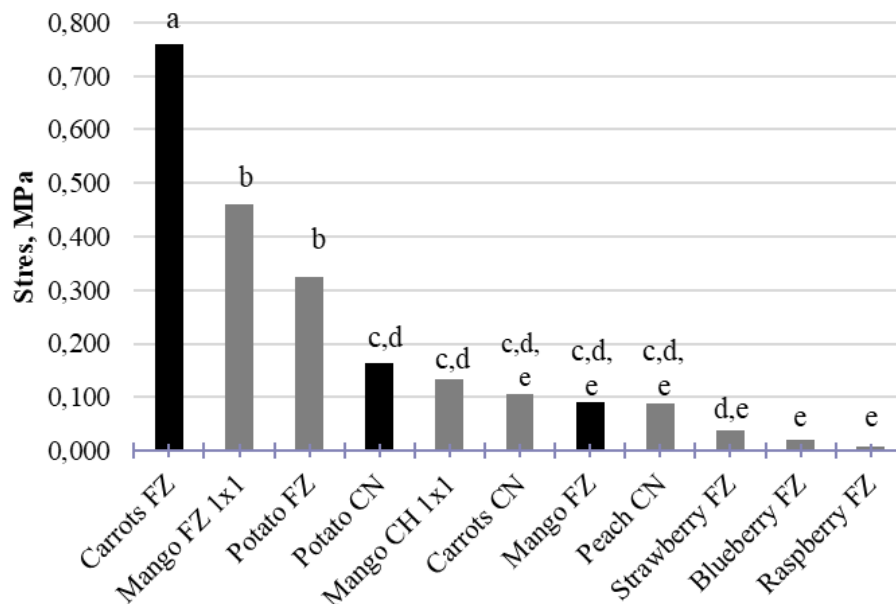
Figure 33 Bio-yield stress of different coarse particles determined by puncture test using 5 mm probe (B) (Note: Different letters indicate significant difference at 95% confidence level.).
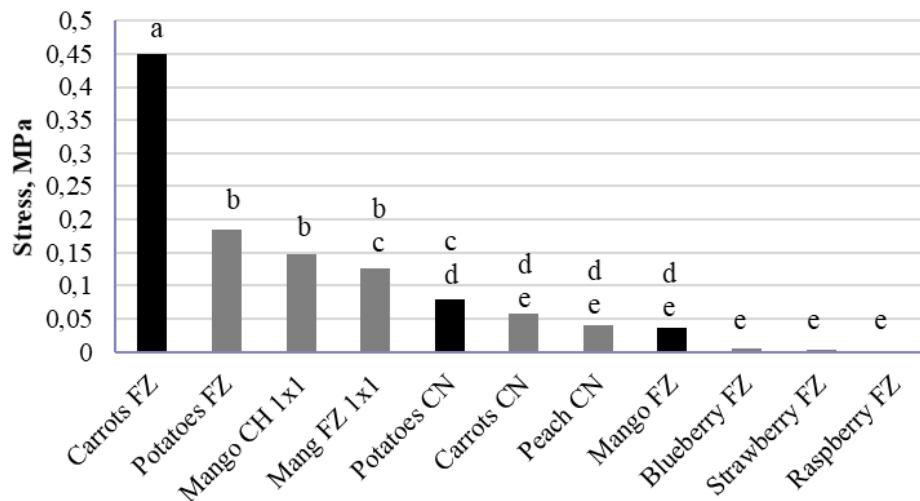
Figure 34 Bio-yield stress of different coarse particles determined by compression test using 36 mm cylindrical probe.
(Note: Different letters indicate significant difference at 95% confidence level.).

The trend on the single compression (Figure 32 and 33) and puncture tests (Figure 34) are similar, wherein thawed carrots (Carrots FZ) had the highest value of bio-yield stress, followed by thawed potatoes (Potato FZ) and thawed mango (Mango FZ 1x1).

Generally, the values for bio-yield stress measured using 2 mm probe is higher compared to the other values using other probes. The stress, which is inversely proportional to the contact area, is very low in 2 mm probe (almost 3% of the particle surface area), and for 5 mm probe the contact area is around 20% of the particle surface area. In processing though, stress of whatever form is applied to the whole surface area of the particle suspended in liquid. Though bio-yield stress measured in compression test is expected to be closer to actual stress in the processing, its correlation with values from puncture test would give alternative test that eliminates the steps in estimating contact area of compression.

The differences of mechanical properties and texture among particles sample as biological materials are influenced by the anatomy of plant tissues, cells size, shape and stacking. Moreover, the thickness and strength of the cell walls and by cell adhesion mechanisms affected such properties also. (Chanliaud *et al.,* 2002; Waldron *et al.,* 2003). In addition, Lasztity et al. (1992) also enumerated other factors for the varying mechanical properties of fruits and vegetables:

- type and variety maturity and the quality of raw product
- the amount of handling between harvesting and processing
- the treatment before freezing and the technology of freezing
- storage time and temperature - thawing procedure

The criteria in choosing the representative particles for the pilot scale experiment are the following:

 a. three particles with distinctly different sensitivities indicated by mechanical properties
 b. readily available
 c. cost efficient.

Frozen-thawed carrots, and mango and canned potatoes were chosen to be involved in the pilot scale experiment (see Figure 35, Table 12).

Figure 35 Particles involved in the experiment – thawed carrots (Carrots FZ, left), thawed mangoes (Mango FZ, center) and canned potatoes (Potato CN, right).

Table 12 Mechanical properties of frozen-thawed carrots, frozen-thawed mango and canned potatoes (n=10).

Parameter	Carrots FZ	Mango FZ	Potato CN
Maximum stress (10% strain), MPa	0.007 ± 0.004	0.003 ± 0.003	0.034 ± 0.010
Maximum stress (20% strain), MPa	0.023 ± 0.006	0.006 ± 0.002	0.077 ± 0.019
Modulus (10% strain), MPa	0.06 ± 0.06	0.02 ± 0.02	0.16 ± 0.10
Modulus (20% strain), MPa	0.09 ± 0.04	0.04 ± 0.01	0.56 ± 0.12
Cohesiveness (10% strain), %	0.71 ± 0.05	0.76 ± 0.03	0.66 ± 0.05
Cohesiveness (20% strain), %	0.62 ± 0.05	0.64 ± 0.05	0.41 ± 0.07
Corrected chewiness (10% strain)	0.45 ± 0.31	0.18 ± 0.16	1.76 ± 0.61
Corrected chewiness (20% strain)	1.09 ± 0.39	0.33 ± 0.10	2.30 ± 0.90
Bio-yield stress (2 mm probe), MPa	1.619 ± 0.676	0.065 ± 0.020	0.218 ± 0.052
Bio-yield stress (5 mm probe), MPa	0.759 ± 0.254	0.091 ± 0.050	0.163 ± 0.035
Bio-yield stress (36 mm probe), MPa	0.451 ± 0.173	0.037 ± 0.023	0.079 ± 0.022

However, it should be noted that these three particle samples have already their own variation in size and shape as the raw material (see Table 13). This could interfere the effect of such studied unit operations when the results were analyzed. The assumption though is that the variability of the sample is not affected by the processing.

Clearly, there are several factors that are needed to be considered in the mechanical test of food particles. It is possible that the values obtain could change if samples are also sourced and handled differently at different conditions. Nevertheless, the tests could show relative differences among samples that could be correlated to the way they will also change their size and shape due to processing.

Table 13 Morphological properties of frozen-thawed carrots, frozen-thawed mango and canned potatoes.

Parameter	Carrots FZ, n=247	Mango FZ, n=120	Potato CN, n=141
Number of particles per 100 g	315 ± 6	80 ± 5	141 ± 6
Mean CE Diameter, mm	8.13 ± 2.18	11.43 ± 6.00	10.96 ± 2.76
Mean circularity	0.613 ± 0.144	0.267 ± 0.132	0.757 ± 0.087
Mean elongation	0.243 ± 0.167	0.342 ± 0.157	0.259 ± 0.139
Mean convexity	0.892 ± 0.069	0.638 ± 0.118	0.966 ± 0.173

Note: The mean standard deviation is calculated from three (3) trials each of two of the treatments.

4.2 Effect of different processing operations to particle morphology

The size and shape of selected particles sample - thawed diced carrots, thawed diced mangoes, and canned diced potatoes with different mechanical properties were quantified using the image analysis method. These particles are subjected to processing conditions such as agitation, passing through wing rotor pump and restriction pipe to allow some breakage.

There are three (3) processing units involved in the experiment – agitation, pumping, and passing through the restriction pipe.
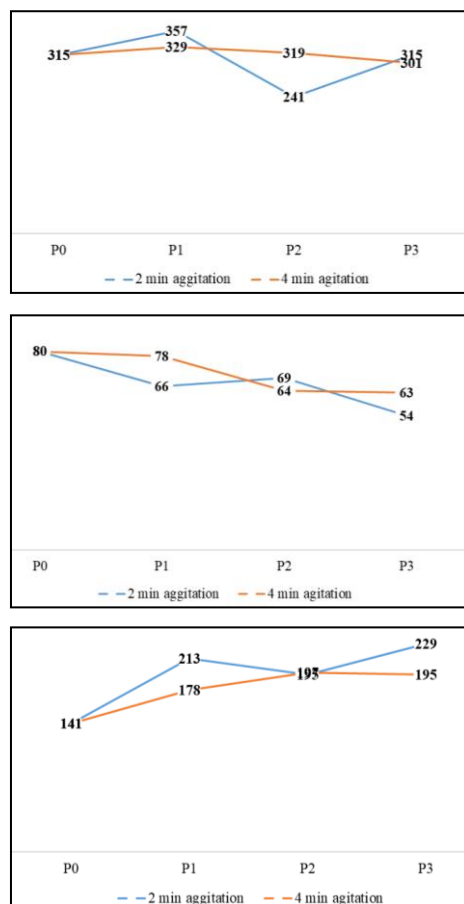
Figure 36 Number of carrot particles (top), mango (center), potato (bottom) per 100 g analyzed in the image analysis.

44

Figure 36 shows the average number of particles analyzed per 100 g of each sample and from each sampling point. The values for the size and shape of the particles are presented in Appendix D. It could be observed that carrots, mango and potato have different trend. Carrots had fluctuating number of particles across all the sampling points, though if considering the particles with 4 minutes agitation, the particle count is consistent. Mango particles had decreasing number of particles from Point 0 to Point 3, while it is reverse for potatoes which increased in particle count. This also gives the idea if the particles become smaller or bigger in the images, or if particles become heavier. Details of while are discussed in the succeeding parts.

The % change in particle size and shape parameters indicate the extent of breakage because of processing. The higher the degree of difference, the higher the changes on the particle's physical characteristics due to the treatment. It can be noted though that the variation within the samples, and sampling errors can also be carried over in this value, so it is important to take these into account. The mean values are also considered to indicate the direction of change, and this can be seen in the trend plot provided by the Morphologi 4-ID. Negative (-) means decrease in the mean of the parameter, while positive (+) indicates increase in value.

$$\textbf{Equation 5} \qquad \% \ \textit{change in parameter} = \frac{Parameter_{after} - Parameter_{before}}{Parameter_{before}}$$

The numerical values of the % change in size and shape of the particles are presented in Appendix E.

4.1.3 Effect of agitation

The effect of agitation to the size and shape parameters of the particles is examined. Sample particles before agitation obtained at Point 0, and sample after agitation at Point 1 are compared. Based on the analysis of the % change in particle characteristics due to agitation, the potato changed the most among the sample particles in terms of CE diameter after 2 minutes and 4 minutes of agitation. (see Figure 37).
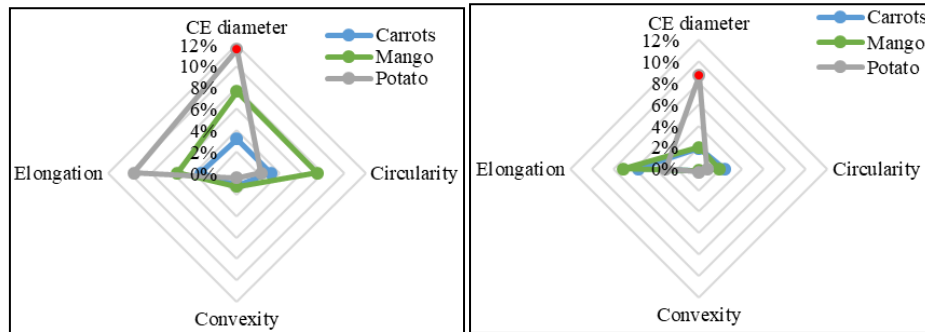
Figure 37 %Change on particle size and shape due to 2 minutes agitation (left) and 4 minutes agitation (right).

The agitation time applied to the particles was kept up to minimum 2 – 4 minutes. However, as mechanical treatment, it could still cause change in particle morphology to some extent. The potato reduced its size after agitation (see Figure 38), while other particles did not change significantly.

.a.

b.

c.

.
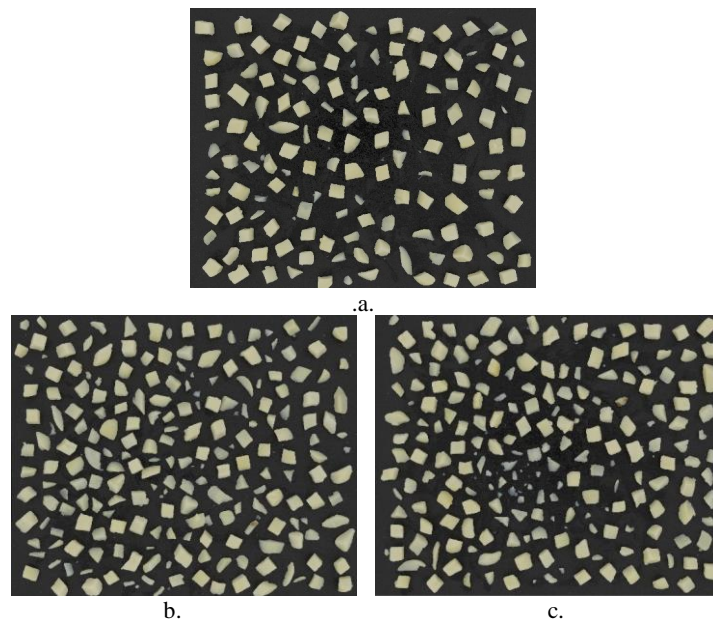
Figure 38 Potato particles sampled at Point 0 (a), at Point 1 after 2 minutes agitation (b) and at Point 1 after 4 minutes agitation (c).

Similar study is done by Bouvier et al. (2011) to develop a model to predict particle breakage due to attrition. Controlled experiment is also done, and they used roundness, which is also the same as circularity parameter, and aspect ratio which is the reciprocal of elongation parameter are used to determine particle breakage. According to their study, the number impeller rotation and Froude number which is related to the vortex of the moving fluid influence the breakage of particles. However, no comparison among particles is done because only one type of particle (gel with known mechanical stress) is used. Nevertheless, the study implied that agitation could cause breakage to particles due to its collision with the tank wall and blade.

4.1.4 Effect of pump

Among the available pumps, the wing rotary pump is known to have the most gentle treatment. Based on the product portfolio of Tetra Pak, it is commonly used in sensitive liquids with solids or large particles, and viscous products.
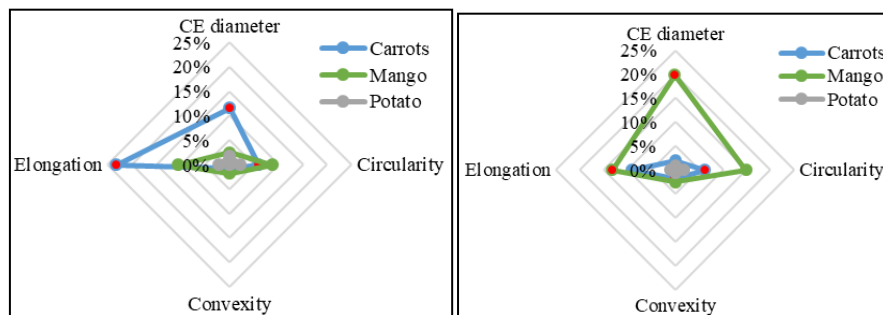
Figure 39 %Change on particle size and shape due to pump at 2 minutes agitation (left) and 4 minutes agitation (right).

Sample particles before pump or after agitation obtained at Point 1, and sample after pump at Point 2 are compared. It could be observed that there is no consistent trend on the % change on morphology among the sample particles at different agitation time. (see Figure 39)

Carrots had dominant change after 2 minutes agitation (-23.11% in elongation, +6.06% in circularity and +11.42% in CE diameter). Upon examining the values of the mean size of these particles, it showed that carrots increased in size from before and after pump. This is not expected because there are no known phenomena that could explain the increase in size of carrots due to pumping. It is then attributed to the movement of particles from the agitation tank to the pump, and sampling method. Even though there is continuous agitation during pumping, large particles sink faster to the bottom of the agitation tank and are pulled by the

47

pump with running motor having 10 Hz frequency. This could explain the apparent increase in size of carrots (see Figure 40).
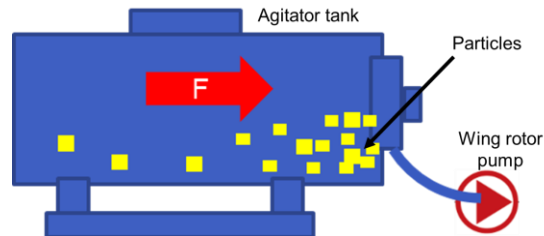
Figure 40 Illustration showing how particles are pulled by the pump from the agitator tank.

Similarly, mango particles also significantly increased in size (+19.74%) after 4 minutes agitation, and broken particles are also observed (see Figure 41). With a possible error due to bigger particles being pulled by pump at Point 2, the effect of pump in the morphology in mango is also not clear. This is mainly caused by the variation of size and shape in the raw materials. In other words, there are not only 1 cm^3 size of particle but also the smaller size of particle fraction contained in the raw material.

a.   b.
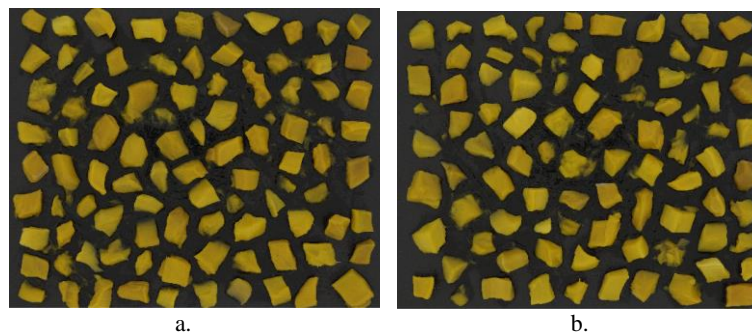
Figure 41 Mango particles with 4 minutes agitation sampled at Point 1 (a.) and Point 2 (b.)

More pronounced changes due to treatment could be observed if particles had uniform dimensions in order to measure the appropriate change after treatment, disregarding the variation on particle size of starting material.

On similar study by Rahardjo (1992), uniform size and shape (cube, sphere and cylinder) of boiled potatoes are analyzed after undergoing pumping. The broken particle fraction is used as indicator of breakage, and it is affected by particle volumetric fraction and fluid turbulence. The density difference of particle and fluid, and direction of the flow had no significant effect on breakage.

4.1.5 Effect of restriction pipe

Appropriate agitation time, and type of pump are decided in order to have more amplified effect of pipe. Sample particles before the restriction pipe or after the pump obtained at Point 2, and sample after the pipe at Point 3 are compared. From Figure 42, it could be observed that carrots had significantly higher % change in elongation: +17.71% and + 9.62% after the treatment among the sample particles at 2 and 4 minutes agitation time respectively.
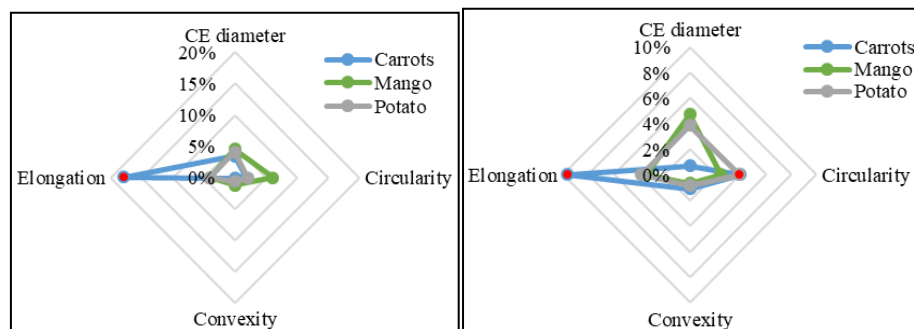
Figure 42 % Change on particle size and shape due to restriction pipe at 2 minutes agitation (left) and 4 minutes agitation (right).

It is possible that this result was already affected by unevenness of particle in the tank of carrots after the pump (Point 2). At this sampling point, the particles are relatively bigger because they sank faster and is pulled by the pump suction. This gave more circular/square-ish shape relative to the smaller particles gathered at after the restriction pipe (Point 3). In addition, the circularity of potato also increased to some extent by 3.95%. Though the changes in morphological properties of mango were not significant, it should be noted that this particle was treated differently from the potato and carrot particles. Mango particles were passed through restriction pipe with 26 mm inner diameter, while the others were in 16 mm. inner diameter restriction pipe.

Through like the other operations that could cause morphological changes in the particles, passing through restriction pipe could also deliver changes due to some external forces like particle-particle collision, particle-wall contact and fluid-particle interaction. Kravchenko et al. (2016) analyzed a similar system of sudden contraction and expansion, and these velocity gradients along this system. The increase in velocity at the inlet of the restriction pipe is larger compared to outlet. According to literature survey by Trägårdh (2019), this could cause the tendency for the particles to drag apart. However, this might not be noticeable in the morphological change of particle, given the set up. The smaller pipe had a length of 0.1 m^{-1}, which is way shorter relative to the flow rate of the particle-liquid mixture that is passing through.

4.1.6 Effect of the overall process

The effect of the overall processing is also examined. Sample particles before the processing (Point 0), and sample after all the processing at Point 3 are compared. In this case, if any errors in sampling method occurred in obtaining samples at Points 1 and 2, these are not taken into account in this comparison.
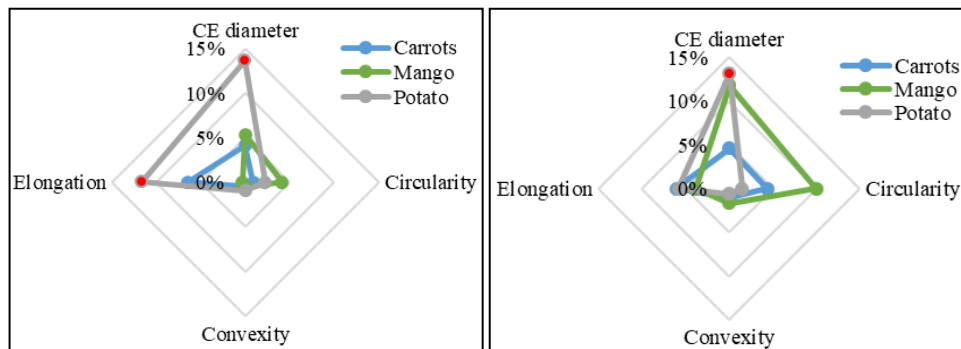
Figure 43 Degree of difference on particle size and shape distribution due to overall processing at 2 minutes agitation (left) and 4 minutes agitation (right).

Figure 44 Potato particles sampled at Point 0 (no processing).

.b.   c.

Figure 45 Potato particles sampled at Point 3 after 2 minutes agitation (b) and at Point 3 after 4 minutes agitation (c).

Figure 43 shows that the trend of the three particles are consistent both after 2 and 4 minutes of agitation. Potato particles exhibit the highest % change in particle morphology, while carrots changed the least. Based on image analysis, from Figure 41, the potatoes decreased in size in terms of its CE diameter and decreased in circularity (more deviant to circle). It is possible that this significant change in size and shape of potato is the effect of agitation, because the pump and restriction pipe caused no significant change in its morphology. Mangoes showed high values in the %change in morphological parameters, however this change is not statistically significant because relatively fewer particles per image frame are analyzed compared to the carrots and mango.

4.1.7 Particle breakage

In morphological perspective, they also behaved differently in the process given their difference in nature. Figure 45 shows images of particles that could explain their probable mechanism of breakage.
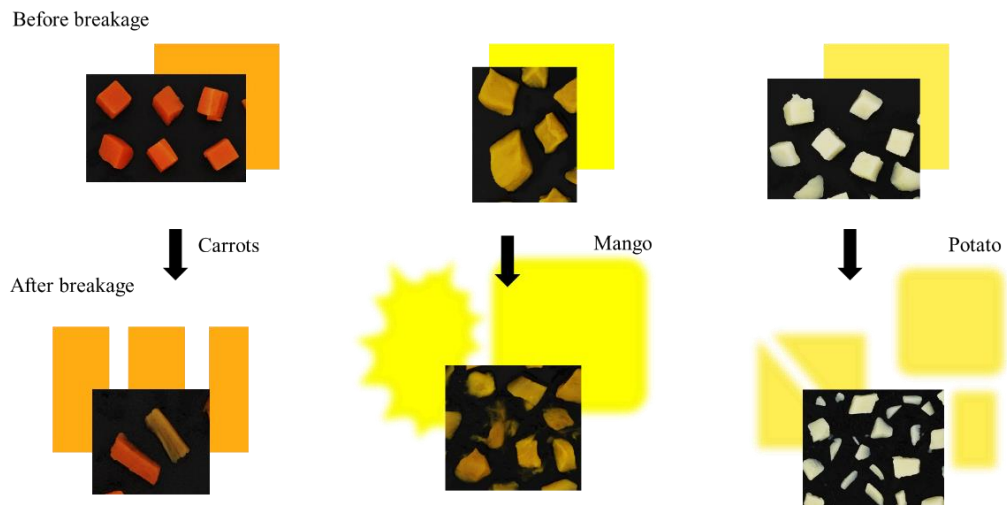
Figure 46 Mechanism of particle breakage.

The particles had different mode of breakage. It could be explained by their biochemical structure and their difference as different species. Carrots have the more tendency to break along the orientation of its fibers, and usually the more sensitive part is at the core. Mango breaks by softening its tissue, its structure is destroyed, and the fiber pulps could protrude. From its intact or more rigid cubic or rectangular prism form, it could soften, and the protruding fibers make it bigger when projected in the frame. Canned potatoes also break by fracture and abrasion. Fracture leads to smaller particles, and abrasion gives very small particles.

4.2 Comparison with sieving technique

The company's existing method of analysis for food products with suspended particles is by sieving. The proposed methods of mechanical tests and image analysis are attempts to have tests that could be able to be used in correlation studies, and prediction models in the future.
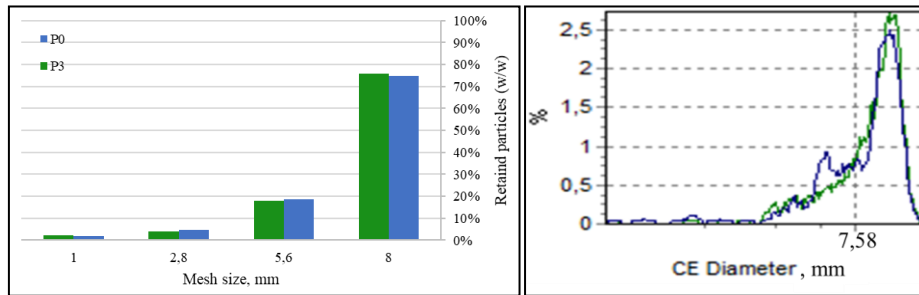
Figure 47 Graphs of particle size distribution of carrots using sieving technique (left) and image analysis (right).
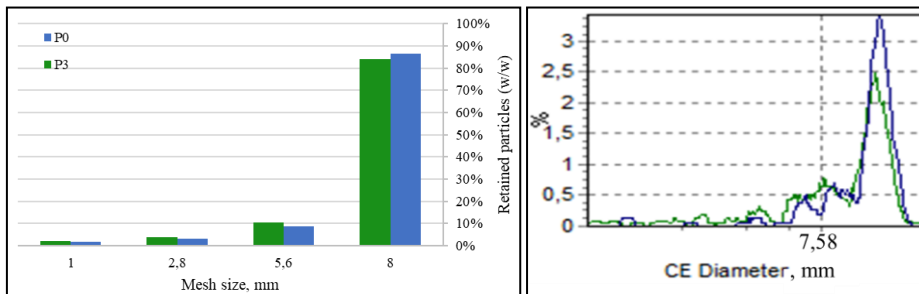
Figure 48 Graphs of particle size distribution of potato using sieving technique (left) and image analysis (right).
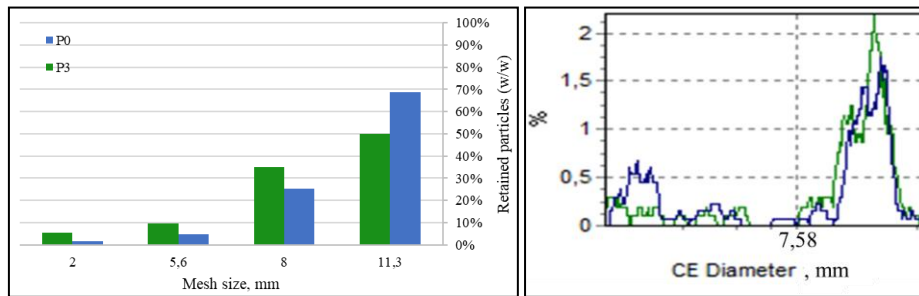
Figure 49 Graphs of particle size distribution of mango using sieving technique (left) and image analysis (right).

Sieving and image analysis are both particle characterization techniques that could provide particle size distribution. However, the former is based on mass, while the latter is based on frequency of particle size as CE diameter.

53

Both the two techniques had similar results for carrots, where the difference in curves before and after treatment is not noticeable (see Figure 47). To some degree, potatoes also showed increase in smaller sizes after the treatment, and this is shown in both techniques (see Figure 48). Mangoes changed in size according to both graphs, but in different trend (see Figure 49). Based on sieving, there is increase in smaller particles; while in image analysis the smaller particles decreased. This discrepancy is expected in mangoes because broken particles are detected differently in both techniques. For image analysis, the breakage leads to larger CE diameter of particles due to the protruding fibers and softened structure; while for sieving analysis, these broken particles are soft enough to pass through the sieve. One important assumption in sieving is that the particles should have low elongation values and high circularity values. In other words, rod shaped particles, and long fibers are difficult to analyze using this technique. The sieving method for mango is challenging because the particles should be handled gently to avoid further destruction of particles.

In conclusion, the existing sieving analysis and image analysis gave similar levels of relative change in size parameter by qualitative evaluation of the cumulative graphs. Sieving is still considered as a rapid method of measuring particle breakage; however, it could not measure shape parameters. This feature can be provided by image analysis which can be used as complementary method to understand mechanism of breakage. For more detailed comparison of the characterization techniques involved in this study, see Table 14.

54

Table 14 Comparison of the particle characterization techniques involved in this study.

Parameters	Separation technique	Mechanical tests		Imaging analysis
	Sieving analysis	Texture Profile Analysis (TPA)	Single compression and puncture	
Principle	Gravimetry	Vertical force	Vertical force	
Apparatus	Stack of test sieves	Texture analyzer	Texture analyzer	Digi-Eye (image capturing) Morphologi 4-ID (image analysis)
Data that could be obtained	Mass based particle size distribution	Hardness Maximum stress Modulus Springiness Cohesiveness Chewiness	Bio-yield stress Ultimate strength Break point	- Size parameters - Shape parameters - Comparison features - Number based or volume-based distribution curves - Other statistical tools
Particle being analyzed	Washed and drained particles	Individual particles (minimum of 8 mm)	Individual particles (minimum of 8 mm)	Washed and drained particles
Time consumption	Simple and cost efficient	Simple, fast and cost efficient	Simple fast and cost efficient	Takes time in sample dispersion and separation of mixed particles
Requirements and special handling	- Should be clean and free from damage - Requires gentle washing, but it could affect the weight of particles	- Requires measurement of individual dimensions; challenging for particles with changing surface area through time		- Requires gentle handling of particles; more sensitive particles are easily affected by handling - Requires more replications, well dispersed samples, and good sampling technique due to variation of sample - Images of the particles should be sharp (not blurred), has good

Limitations	- Issues with adhesive particles - Assumption of regular sized particles - Brittle particles may break, and abrasive particles may wear off	- Particles should have smooth and straight surface - Good results with particles having max force of at least 20 g	- Table effect - If the studied particle have almost similar texture, by using 2 mm probe could not show the difference among sample.	contrast and good lighting - 2D image; thickness of particle is not taken into account; particles could be converted into sphere equivalent - Overlap and attached particles are eliminated in the analysis - Better results with opaque particles

5 Conclusion

This section enumerates the conclusion derived from the results of the study.

The following are concluded based on the results of the study:

1. Particle strength can be measured in three different ways. In this study, this property was measured using double compression at the elastic limit and compression and puncture up to the bio-yield point; however, the results have different trend. For example, canned potato particles show high levels of particle strength measured at the elastic limit, while carrot particles at the bio-yield point. These results were sought to be correlated to the results of the morphological analysis.

2. Even the pilot scale experiment conditions were intended to be harsher than in the real food processing conditions, the mango and carrot particles did not break significantly based on image analysis. Correlation of the results of mechanical test and image analysis cannot be done because not all the particles tested (2 out of 3) did not significantly break. The results of image analysis on the effect of pump and restriction pipe are not conclusive because of the uneven distribution of particles in the agitator.

3. No conclusion can be derived on the comparison of the three particles tested. Based on the availability of the raw material, thawed mangoes were treated with the different test conditions from the other particles.

4. For more rapid measurement of particle breakage, the existing sieving analysis is still recommended. However, this method is limited to mass and volume-based particle size distribution. For cases that good quality images of particles are desired, image analysis is suggested to be done. Aside from particle size distribution, shape parameters can be obtained that are helpful on understanding mechanism of breakage.

6 Recommendations for Future Research

This section enumerates the recommendations and areas for future research derived from the results of the study.

The following are recommendations based on the results and findings of the study:

1. The use of apparatus for mechanical tests that could measure smaller forces is recommended.
2. Apply the same study using other types of particles in order to have more points in the correlation.
3. Other forms of particle breakage like shearing and measurement of stress from fluid can also be examined for correlation studies.
4. For modelling studies, food sample model (e.g. standardized cubic gel particles) could be used in the test instead of using real food sample in order to avoid variation within the sample. In this case, the change in particle morphology due to the processing is amplified.
5. In order to investigate the effect of restriction rig, the possible future work that could be done are to provide harsher treatment such as using smaller restriction rig, to increase the fluid flow rate.
6. Perform the same study and focusing on other unit operations such as agitation, pumping, passing through valve, and heat treatment. If possible, one-unit operation at a time is recommended to avoid interference of the effects of other operation to the particles.

References

Abbott, J. A. (1999). Quality measurement of fruits and vegetables. *Postharvest Biology and Technology*, 15(3), pp. 207-225.

Akker, J. (1999). Principles and Methods of Developmental Research. Dordrecht: Kluwer Academic Publishers. Available at: https://pdfs.semanticscholar.org/e1a5/7b0704bd9dd2417fb579ce1bcb5b09 fde26a.pdf.

Analytic Method Development and Validation. (2009). Particle Science-Drug Development Services (5). Available at: https://www.particlesciences.com/news/technical-briefs/2009/analytic-method-development-and-validation.html.

Aviara, N. A., Shittu, S. K. & Haque, M. A. (2007). Physical properties of guna fruits relevant in bulk handling and mechanical processing. International Agrophysics, 21, pp. 7-16.

Bourne, M. C. (1980). Texture evaluation of horticultural crops. *Horicultural Science*, 15(1): pp. 51-57.

Bourne, M. C. (2002). Food texture and viscosity: concept and measurement. London:Elsevier.

Bouvier, L., Moreau, A., Linh, A., Fatah, N., & Delaplace, G. (2011) Damage in Agitated Vessels of Large Visco-Elastic Particles Dispersed in a Highly Viscous Fluid, *Journal of Food Science*, 76(5), pp. 384-391.

Cantu-Lozano, D., Rao, M. A. & Gasparetto, C. A. (2000). Rheological Properties on Non-cohesive Apple Dispersion with Helical and Vane Impellers: Effect of Concentration and Particle Size, *Journal of Food Process Engineering*, 23, pp. 373-385.

Casteren, W. V. (2017). The Waterfall Model and the Agile Methodologies : A comparisonnby project characteristics, *Academic Competences in the Bachelor assignment,* pp.1.

Chandra, M. V. & Shamasundar, B. A. (2015). Texture Profile Analysis and Functional Properties of Gelatin from the Skin of Three Species of Fresh Water Fish, *International Journal of Food Properties*, 18:3, pp. 572-584.

Chanliaud, E., Burrows, K. M., Jeronimidis, G., and Gidley, M. J. (2002). Mechanical   properties of primary plant cell wall analogues. Planta ,215, pp. 989-996.

Chen, J. & Rosenthal, A. (2015). Food Texture and Structure, *Woodhead Publishing Series in   Food Science, Technology and Nutrition*, (1), pp. 3-24.

Dal, Y. L. and Light, J. M. (2014). Food Texture Design and Optimization. UK: John Wiley &   Sons, Ltd.

Faber, T. J., Jaishankar, A., & Jaishankar, G.H. (2016). Describing the firmness, springiness   and rubberiness of food 2 gels using fractional calculus. Part I: Theoretical   framework. *Food Hydrocolloids*, 62.

Foegeding, E. A., Daubert, C. R., Drake, M. A., Essick, G., Trulsson, M., Vinyard, C. J. & Van   De Velde, F. (2011). A comprehensive approach to understanding textural properties of semi- and soft-solid foods. *Journal of Texture Studies*. 42(2), pp. 103–129.

Gholami, R. et al. (2012). Determination of Physical and Mechanical Properties of Zucchini   (summer squash). *Agricultural Engineering International: The CIGR e-journal*, 14(1),   pp. 136-140.

Guinaed, J. X. & Mazzucchelli R. (1996). The sensory perception of texture and mouthfeel,   *Trends in Food Science and Technology*, 7(7), pp. 213-219.

Hawkins, A. E. (1993). The Shape of Powder-Particle Outlines. Wiley, New York.

Gunasekaran, S. (2001). Nondestructive Food Evaluation: Techniques to Analyze Properties and Quality. New York: Marcel Dekker, Inc.

Johansson, J. & Vall, J. (2011). Jordmaterials kornform. Inverkan på Geotekniska Egenskaper, Beskrivande   storheter,   bestämningsmetoder. Examensarbete. Avdelningen för Geoteknologi, Institutionen   för Samhällsbyggnad och naturresurser. Luleå Tekniska   Universitet, Luleå.

Kilickan, A., and M. Gunner. (2008). Physical properties and mechanical behavior of olive fruits (*Oleaeuropaea L.*) under compression loading. *Journal of Food Engineering*, 87(2): pp. 222–228.

Kumar, A. (2012). Method development and validation. Chronicles of Young Scientists, 3(1), pp. 3-9.

Lasztity, R., Sebok, A. & Major J. (1992). Textural properties of fruits and vegetables and their changes during freezing and storage at low

temperatures. *Periodica Polytechnica Chemical Engineering,* 36(4), pp. 225-238.

Li, Z., Miao, F. & Andrews, J. (2017). Mechanical Models of Compression and Impact on Fresh Fruits. *Comprehensive Reviews in Food Science and Food Safety*, 16, pp. 1296 – 1309.

Lu, R., and Abbott, J. A. (2004). Chapter 5. Force deformation techniques for measuring texture. In Texture in Food, Vol. 2: Solid Foods, ed. D. Kilcast. Cambridge, England: Woodhead Publishing Limited.

Lu, R., Srivastava, A. K., & Beaudry, R. M. (2005). A New Bioyield Tester for Measuring Apple Fruit Firmness. *Applied Engineer in Agrculture*, 21(5), pp. 893-900.

Lu, R. (2013). Principles of Solid Food Texture Analysis. USA: Woodhead Publishing Limited.

Lucka, M. & Hanke, T. (2016). Sieve Analysis Different sieving methods for a variety of applications, *Solution in Milling and sieving*

Lustig, I. & Berstein, Z. (1987). An improved firmness tester for juicy fruit. *Horticultural Science*, 22(4), pp. 653-655.

Malvern. (2015). A Basic Guide to Particle Characterization, Whitepaper. UK: Malvern Instruments Limited.

Merkus, H. G. (2009). Particle Size Measurements: Fundamentals, Practice, Quality. The Netherlands: Springer Science+Business Media B.V.

Meloy, T. P. (1980). Advance Particulate Morphology, pp- 66–76.

Meloy, T. P. (1997). Powder Technology, 16, pp. 233–253.

Mohsenin, N. N. (1986). Physical Properties of Plant and Animal Materials , Second Updated and Revised Edition. New York: Gordon and Breach Science Publishers.

Mora, C. F. and Kwan, A. K. H. (2000). Sphericity, shape factor, and convexity measurement of coarse aggregate for concrete using digital image processing. *Cement and Concrete Research.* 30(3), pp. 351-358.

Morphologi 4-ID user manual. Malvern Panalytical, Enigma Business Park, Grovewood Road, Malvern, Worcestershire WR14 1XZ, UK.

Nishinari, K. et al. (2013). Parameters of Texture Profile Analysis. *Food Science, Technology and Research*, 19(3), pp. 519-521.

Ourecky, D. K. & Bourne, M. C. (1968). Measurement of strawberry texture with an Instron machine. *American Society for Horticultural Science*, 93, pp. 317-325.

Pallottino, F., C. Costa, P. Menesatti, & M. Moresi. (2011). Assessment of the mechanical properties of Tarocco orange fruit under parallel plate compression. *Journal of Food Engineering*, 103(3), pp. 308-316.

Rahardjo, B. (1992). Analysis of damage to food particles during pumping. (Electronic Thesis or Dissertation). Available at: https://etd.ohiolink.edu/.

Rahardjo, B. & Sastry, S. K. (1993). Food particle damage and particle-wall collisions during pumping of solid-liquid mixtures, *Food and Bioproducts Processing: Transactions of the Institution of Chemical Engineers*, 71(4), pp. 242-250.

Rahman, M. S. & Al-Farsi, S. A. (2005) Instrumental texture profile analysis (TPA) of date flesh as a function of moisture content. *Journal of Food Engineering*, 66, pp. 505–511.

Ravisankar, P., Navya, N., Pravallika, D. & Sri, D. N. (2015). A Review on Step-by-Step Analytical Method Validation, *IOSR Journal Of Pharmacy*, 5(10), pp. 7-19.

Riley, N. A. (1941). Projection sphericity. *Journal of Sedimentary Petrology*. 11(2), pp. 94-97.

Robins, M. M. (2006). *Particle Size Analysis in Food,* John Wiley & Sons, UK: Wiley.

Rodriguez, J. M. (2013). Importance of the Particle Shape on Mechanical Properties of Soil Materials. Luleå University of Technology. Available at: http://ltu.diva-portal.org/smash/get/diva2:999596/FULLTEXT02.pdf.

Roos, Y. H. (1995). Mechanical Properties, *Phase Transition in Food*, pp. 247-270.

Rosenthal, A. J. (2010). Texture Profile Analysis – How Important are the Parameters?, *Journal of Texture Studies* 41, Wiley Periodicals, Inc. pp 672 – 684.

Royce, W. W. (1970) Managing the development of large soft- ware systems. In proceedingsof IEEE WESCON, 8, pp. 328–338.

Savov, A. V. & Kouzmanov. (2009). Food Quality and Safety Standards at a Glance, *Biotechnology & Biotechnological Equipment*, 23(4), pp. 1462-1468.

Singh, K. K. and Reddy, B. S. (2006). Post-harvest physico-mechanical properties of orange peel and fruit. Journal of Food Engineering, 73, pp. 112-120.

Snedecor, G. W., and Cochran, W. G. (1980.) *Statistical Method*, Seventh Edition. Ames, Iowa: The Iowa State University Press. Sugimoto, K., Legami, C.

M., Lida, S., Naito, M., Tamaki, R. & Minagi S. (2012) New image analysis of large food particles can discriminate experimentally suppressed mastication. *Journal of Oral Rehabilitation,* 39(6), pp. 405-410.

Tiago, B., Luis, G., Marta, G. C., Anna, C., Jason, A., Jordi, G. M. & Maria, H. (2016). Textural properties of different melon fruit types: sensory and physical-chemical evaluation. Sci Hortic-Amsterdam, 201, pp. 46–56.

Timm, E. J., Brown, G. K., Armstrong, P. R., and Beaudry, R. M. (1993). A portable instrument for measuring firmness of cherrie and berries. Developing a blueberry firmness standard. *Transactions of the ASAE*, 28(3), pp. 986-992.

Trinh, K. T. & Glasgow S. (2012). On the Texture Profile Analysis Test. Proceedings of the International Conference of Chemeca Wellington, New Zealand, 23-26 September 2012.

Wadell, H. (1932). Volume, Shape, and roundness of rock particles. *Journal of Geology, 40*, pp. 443-451.

Wadell, H. (1933). Sphericity and roundness of rock Particles. *Journal of Geology.* 41(3), pp. 310–331.

Waldron, K.W., Parker, M. L., and Smith, A.C. (2003). Plant cell walls and food quality. *Comprehensive reviews in food science and food safety*, 2, pp. 101-119.

WELMEC. (2013). Guide on the Verification of Drained Weight, Drained Ished Weight andDeglazed Weight. WELMEC 6.8(2).

Yan, Y., Zhang, Z., Stokes, J. R., Zhou, Q. Z., Ma, G. H. & Adams, M. J. (2009). Mechanical characterization of agarose micro-particles with a narrow size distribution. Powder Technology, 192, pp. 122–130.

Appendix A: Work Distribution and Time Plan

The thesis is carried out by the two team members who had similar backgrounds and experiences in Food Technology and Engineering.

Both participated in every activity, performing the project from project planning to reporting together: literature review, mechanical tests of the particles; and analysis of results

Some of the experiments required more than one person to perform at the same time:

- Sample preparation and dispersion for the image analysis
- Setting up the pilot scale experiment
- Sampling at P2
- Cleaning up

Activities	Molina	Hutasingh
Pilot scale experiment	Sampling at P0 and P1	Sampling at P3
Analysis of samples	Sieving analysis	Image analysis

At the pilot scale experiment, the tasks of getting the sample from the rig are clearly divided. Since the sampling at the rig need to be sampled at the same agitator time in order to avoid errors. It means that the sampling of particle should be done simultaneously and fast.

Because the collected samples should be analyzed at most 2 days after the experiment, image analysis and sieving analysis should be done simultaneously.

Regarding the report, even though sections of the report have been written individually at the beginning, finally both team members helped each other to revise and review the entire report.

Activities — Gantt chart (yellow = planned activity period; green columns = milestones)

Activities	19-Nov-18	26-Nov-18	03-Dec-18	10-Dec-18	17-Dec-18	21-Jan-19 (1)	28-Jan-19 (2)	04-Feb-19 (3)	11-Feb-19 (4)	18-Feb-19 (5)	25-Feb-19 (6)	04-Mar-19 (7)	11-Mar-19 (8)	18-Mar-19 (9)	25-Mar-19 (10)	01-Apr-19 (11)	08-Apr-19 (12)	15-Apr-19 (13)	22-Apr-19 (14)	29-Apr-19 (15)	06-May-19 (16)	13-May-19 (17)	20-May-19 (18)	27-May-19 (19)	05-Jun-19 (20)
Presentation of the proposal				■																					
Literature review	■	■	■	■	■																				
Define and set up analysis methods							■	■	■	■	■	■	■	■	■										
Analysis of actual samples													■	■	■	■	■								
Planning of trials																		■							
Application of methodologies to pilot scale																			■						
Data analysis																				■	■				
Report writing and revisions																						■	■		
Submitting thesis to the examiner																									
Presentation of thesis																									

Milestone (green) columns: week 1 (21-Jan-19) "Start of thesis"; week 8 (11-Mar-19) "Midterm presentation"; week 19 (27-May-19) "Submission to examiner"; week 20 (05-Jun-19) "Presentation".

Figure 50. Initial time plan.

Activities	19-Nov-18	26-Nov-18	03-Dec-18	10-Dec-18	17-Dec-18	1 (21-Jan-19)	2 (28-Jan-19)	3 (04-Feb-19)	4 (11-Feb-19)	5 (18-Feb-19)	6 (25-Feb-19)	7 (04-Mar-19)	8 (11-Mar-19)	9 (18-Mar-19)	10 (25-Mar-19)	11 (01-Apr-19)	12 (08-Apr-19)	13 (15-Apr-19)	14 (22-Apr-19)	15 (29-Apr-19)	16 (06-May-19)	17 (13-May-19)	18 (20-May-19)	19 (27-May-19)	20 (05-Jun-19)
						Start of thesis							**Midterm presentation**											**Submission to examiner and opponent**	**Presentation**
Presentation of the proposal			▓																						
Literature review	▓	▓	▓	▓	▓	▓	▓	▓	▓	▓	▓	▓		▓	▓										
Report writing and revisions							▓	▓	▓	▓	▓	▓		▓	▓	▓	▓	▓	▓	▓	▓	▓			
Define and set up analysis methods							▓	▓	▓	▓	▓	▓		▓											
Analysis of actual samples											▓	▓		▓											
Planning of trials														▓	▓										
Pilot scale run																▓	▓	▓	▓						
Application of methodologies to pilot scale																▓	▓	▓	▓						
Data analysis																			▓	▓					
Finalize report and do revisions																					▓	▓			
Submission of thesis to the examiner																									
Presentation of thesis																									

Figure 51 Actual time plan.

Appendix B: Mechanical Properties of the Sample Particles

Table 15 *Texture parameters of sample particles.*

Particle	% Strain		Hardness, g	Stress, MPa	Modulus, MPa	Springi-ness	Cohesive-ness	Corrected Chewiness *
Blueberry FZ	20%	Mean (n=10)	18,64	0,006	0,00	74,89	0,43	0,22
		SD	6,30	0,002	0,00	10,18	0,10	0,11
		CV, %	33,81	33,358	49,31	13,59	22,63	48,61
Carrots CN	10%	Mean (n=10)	254,88	0,022	0,12	81,00	0,66	1,20
		SD	77,85	0,007	0,06	5,37	0,04	0,31
		CV, %	30,54	31,526	49,18	6,62	6,16	25,80
Carrots CN	20%	Mean (n=10)	524,74	0,049	0,34	70,72	0,34	1,22
		SD	131,37	0,014	0,08	11,27	0,07	0,55
		CV, %	25,04	28,339	24,27	15,93	20,95	45,16
Carrots FZ	10%	Mean (n=10)	50,43	0,007	0,06	82,45	0,71	0,45
		SD	22,66	0,004	0,07	9,05	0,05	0,31
		CV, %	44,93	56,720	107,15	10,98	7,29	69,19
Carrots FZ	20%	Mean (n=10)	174,29	0,023	0,09	76,50	0,62	1,09
		SD	62,30	0,006	0,04	7,56	0,05	0,39
		CV, %	35,74	27,740	40,10	9,88	7,60	36,02
Potato CN	10%	Mean (n=10)	339,76	0,034	0,16	78,73	0,66	1,76
		SD	78,05	0,010	0,10	8,09	0,05	0,61
		CV, %	22,97	30,800	62,90	10,28	8,20	34,39
Potato CN	20%	Mean (n=10)	714,58	0,077	0,56	70,70	0,41	2,30
		SD	150,02	0,019	0,12	4,52	0,07	0,90
		CV, %	20,99	24,358	21,07	6,40	16,29	38,89

Potato FZ	10%	Mean (n=10)	102,82	0,010	0,09	87,97	0,81	0,70
		SD	53,90	0,005	0,05	3,56	0,02	0,35
		CV, %	52,42	52,895	54,88	4,04	2,98	49,79
Potato FZ	20%	Mean (n=10)	184,83	0,022	0,11	76,42	0,71	1,21
		SD	69,40	0,007	0,04	7,52	0,06	0,49
		CV, %	37,55	33,238	36,53	9,84	7,69	40,45
Potato CH	10%	Mean (n=10)	144,70	0,015	0,09	80,11	0,77	0,94
		SD	31,30	0,004	0,03	4,67	0,03	0,28
		CV, %	21,63	25,184	32,06	5,83	3,82	29,36
Potato CH	20%	Mean (n=10)	1005,09	0,099	0,92	66,35	0,67	4,49
		SD	386,64	0,035	0,30	7,74	0,03	1,92
		CV, %	38,47	35,679	32,98	11,66	5,06	42,79
Raspberry FZ	10%	Mean (n=10)	2,31	0,001	0,00	80,56	0,55	0,05
		SD	2,59	0,000	0,00	6,21	0,05	0,03
		CV, %	111,93	38,334	50,82	7,70	8,30	52,93
Raspberry FZ	20%	Mean (n=10)	12,75	0,001	0,00	61,65	0,45	0,04
		SD	4,44	0,000	0,00	9,80	0,05	0,01
		CV, %	34,85	31,123	32,56	15,89	10,86	38,03
Strawberry FZ	10%	Mean (n=10)	21,03	0,002	0,01	79,63	0,61	0,09
		SD	7,20	0,001	0,00	3,52	0,05	0,04
		CV, %	34,23	34,130	35,96	4,42	7,70	39,91
Strawberry FZ	20%	Mean (n=10)	48,80	0,002	0,01	69,93	0,55	0,05
		SD	28,12	0,001	0,01	10,42	0,03	0,02
		CV, %	57,62	58,130	64,58	14,90	5,24	42,19
Olives CN	10%	Mean (n=10)	102,49	0,008	0,02	74,98	0,68	0,43
		SD	47,02	0,004	0,01	4,43	0,03	0,21
		CV, %	45,88	45,789	51,52	5,91	5,00	48,45
Olives CN	20%	Mean (n=10)	549,33	0,045	0,23	61,34	0,56	1,54
		SD	194,72	0,016	0,09	6,08	0,05	0,64
		CV, %	35,45	35,447	36,83	9,91	8,39	41,23
Peach CN	10%	Mean (n=10)	59,26	0,006	0,02	88,76	0,75	0,39
		SD	23,70	0,002	0,01	3,62	0,03	0,17
		CV, %	40,00	41,707	34,15	4,08	3,79	43,78

Peach CN	20%	Mean (n=10)	287,91	0,024	0,19	82,43	0,55	1,08
		SD	60,50	0,003	0,04	2,00	0,04	0,17
		CV, %	21,01	12,549	19,83	2,43	7,42	15,97
Mango FZ	10%	Mean (n=10)	62,30	0,003	0,02	84,13	0,76	0,18
		SD	54,15	0,003	0,02	3,62	0,03	0,16
		CV, %	86,91	94,023	96,39	4,30	3,81	90,64
Mango FZ	20%	Mean (n=10)	142,25	0,006	0,04	81,27	0,64	0,33
		SD	54,77	0,002	0,01	4,07	0,05	0,10
		CV, %	38,50	31,497	32,20	5,00	7,50	29,29
Mango FZ 1x1	10%	Mean (n=10)	105,39	0,013	0,08	86,36	0,80	0,87
		SD	28,97	0,004	0,03	3,79	0,02	0,27
		CV, %	27,49	30,348	39,88	4,39	2,92	31,29
Mango FZ 1x1	20%	Mean (n=10)	404,23	0,050	0,42	80,82	0,64	2,52
		SD	146,34	0,016	0,15	3,11	0,02	0,79
		CV, %	36,20	33,049	35,20	3,85	3,83	31,40
Mango CH 1x1	10%	Mean (n=10)	89,04	0,009	0,05	84,51	0,74	0,53
		SD	54,31	0,007	0,04	6,98	0,03	0,36
		CV, %	61,00	73,454	67,23	8,26	4,30	67,37
Mango CH 1x1	20%	Mean (n=10)	277,31	0,031	0,16	78,06	0,54	1,30
		SD	65,57	0,008	0,05	5,22	0,03	0,37
		CV, %	23,64	26,860	30,13	6,69	6,17	28,80

Table 16 Bio-yield stress of sample particles using different probes.

Particle		Bio-yield stress, MPa		
		36 compression probe	2 mm puncture probe	5 mm puncture probe
Blueberry FZ	Mean (n=10)	0,005	0,062	0,020
	SD	0,003	0,041	0,011
	CV, %	75,2	66,3	56,8
Carrots CN	Mean (n=10)	0,058	0,146	0,107
	SD	0,015	0,074	0,024
	CV, %	25,8	50,8	22,2
Carrots FZ	Mean (n=10)	0,451	1,619	0,759

	SD	0,173	0,676	0,254
	CV, %	38,3	41,8	33,5
Potato CN	Mean (n=10)	0,079	0,218	0,163
	SD	0,022	0,052	0,035
	CV, %	28,4	23,9	21,6
Potato FZ	Mean (n=10)	0,184	0,688	0,325
	SD	0,075	0,282	0,157
	CV, %	40,8	41,0	48,4
Raspberry FZ	Mean (n=10)	0,0014	0,017	0,007
	SD	0,00023	0,004	0,002
	CV, %	16,9	24,5	32,8
Strawberry FZ	Mean (n=10)	0,004	0,057	0,037
	SD	0,002	0,051	0,024
	CV, %	56,7	89,3	65,6
Peach CN	Mean (n=10)	0,040	0,098	0,088
	SD	0,010	0,045	0,029
	CV, %	24,0	46,1	33,0
Mango FZ	Mean (n=10)	0,037	0,065	0,091
	SD	0,023	0,020	0,050
	CV, %	61,5	30,5	55,1
Mango FZ 1x1	Mean (n=10)	0,127	0,541	0,461
	SD	0,026	0,385	0,221
	CV, %	20,3	71,3	48,0
Mango CH 1x1	Mean (n=10)	0,147	0,167	0,134
	SD	0,061	0,064	0,038
	CV, %	41,8	38,2	28,1

Appendix C: Pictures of the Sample Particles for Morphological Analysis

2 minutes agitation

P0 (before processing)

P1 (after agitation)

P2 (after pump)

P3 (after restriction pipe)

4 minutes agitation

P1 (after agitation)

P2 (after pump)

P3 (after restriction pipe)
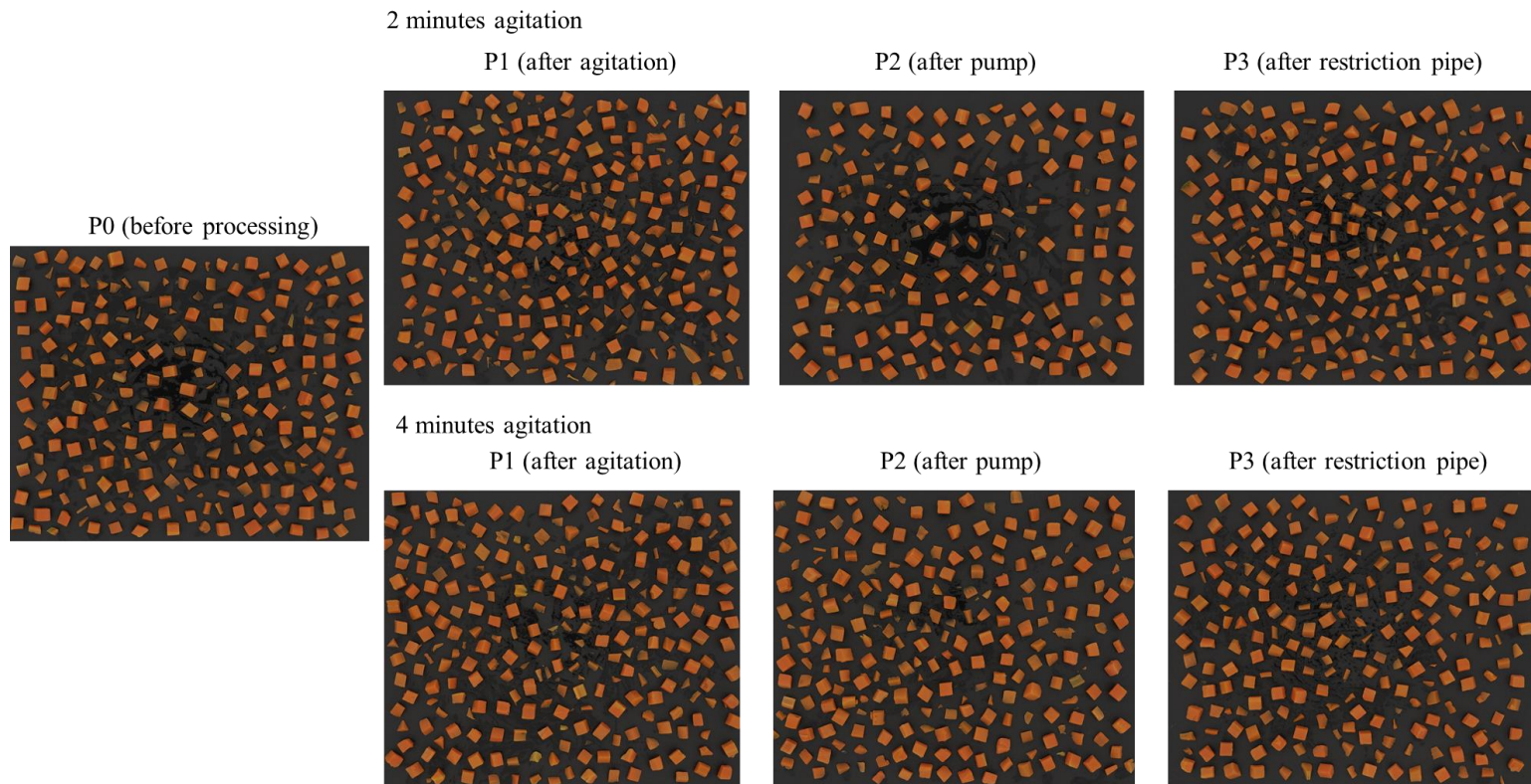
Figure 52 Images of carrot particle samples when subjected to processing.

72

2 minutes agitation

P0 (before processing)   P1 (after agitation)   P2 (after pump)   P3 (after restriction pipe)

4 minutes agitation

P1 (after agitation)   P2 (after pump)   P3 (after restriction pipe)
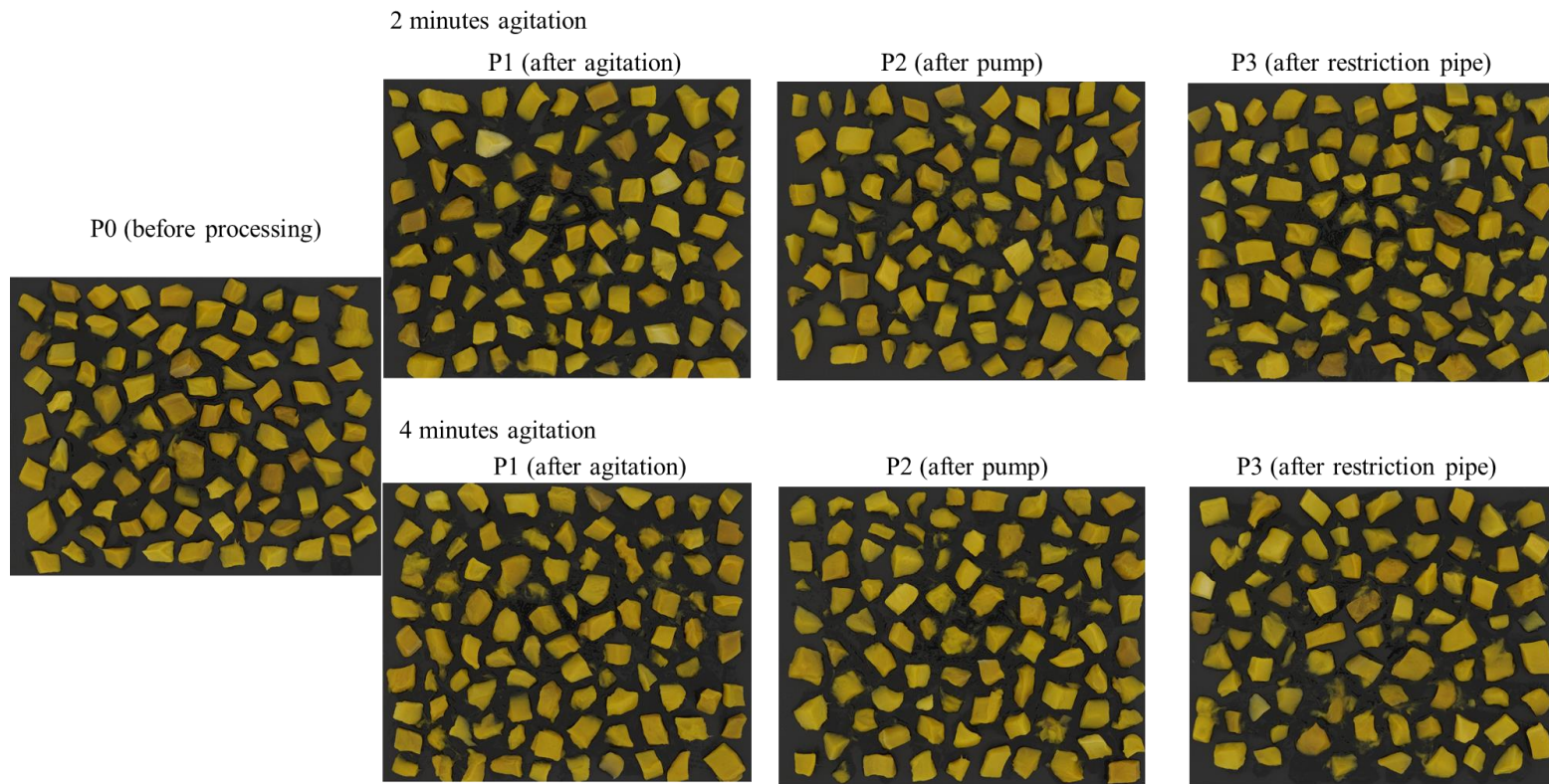
Figure 53 Images of mango particle samples when subjected to processing.

2 minutes agitation

P1 (after agitation) P2 (after pump) P3 (after restriction pipe)

P0 (before processing)

4 minutes agitation

P1 (after agitation) P2 (after pump) P3 (after restriction pipe)
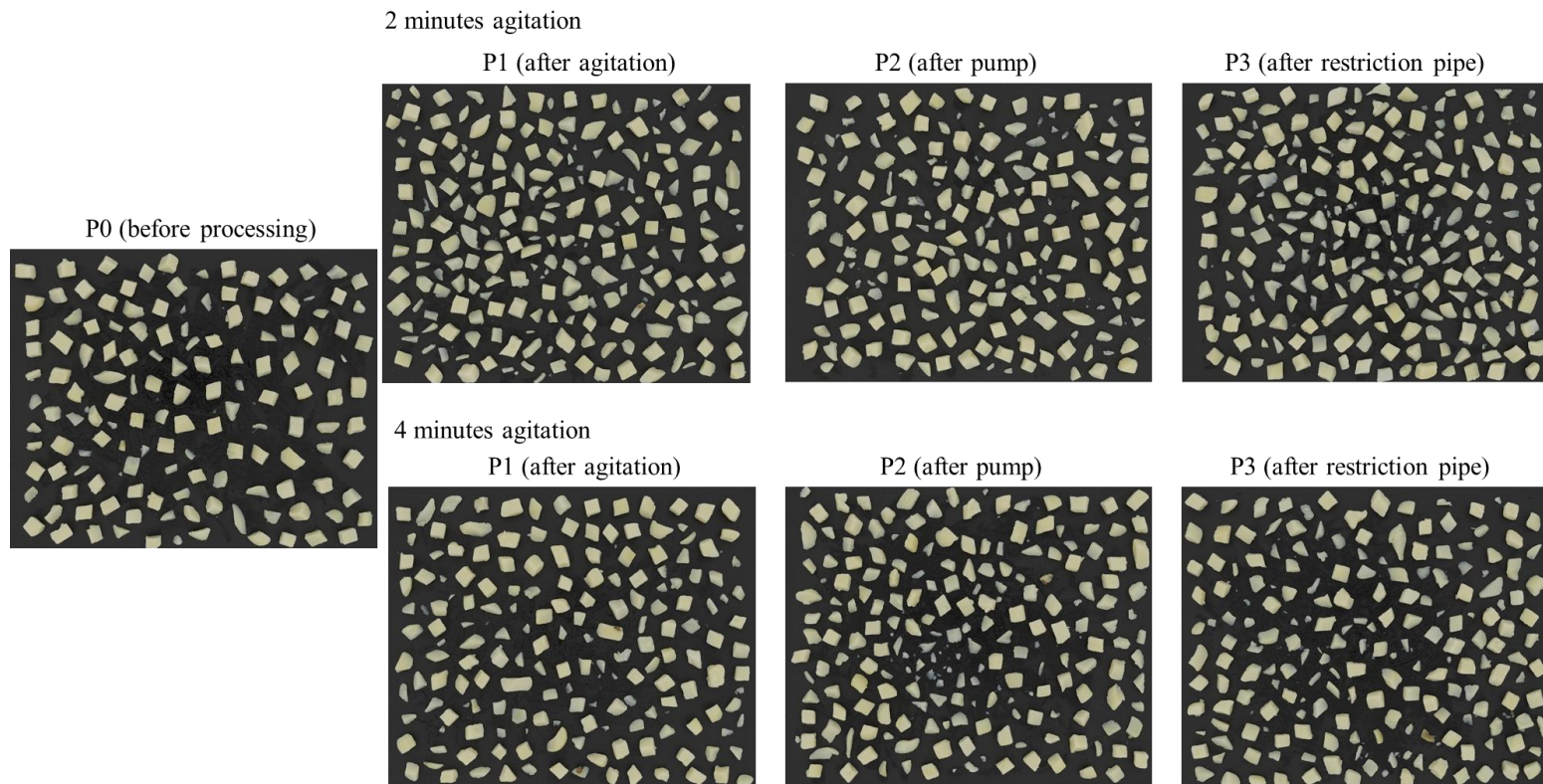
Figure 54 Images of potato particle samples when subjected to processing.

Appendix D: Size and Shape of Sample Particles

Table 17 Size and shape of carrot particles.

Sample Name	# Particles per frame	CE Diameter Mean (mm)	Circularity Mean	Elongation Mean	Convexity Mean
No treatment	247	8.13	0.613	0.243	0.892
2 minutes agitation. collected at P1	268	7.87	0.594	0.251	0.882
2 minutes agitation. collected at P2	181	8.77	0.630	0.193	0.889
2 minutes agitation. collected at P3	232	8.47	0.619	0.227	0.888
4 minutes agitation. collected at P1	247	8.28	0.628	0.229	0.894
4 minutes agitation. collected at P2	239	8.44	0.667	0.208	0.911
4 minutes agitation. collected at P3	226	8.50	0.640	0.228	0.901
Standard deviation	8.115	2.18	0.144	0.167	0.069

Table 18 Size and shape of mango particles.

Sample Name	# Particles per frame	CE Diameter Mean (mm)	Circularity Mean	Elongation Mean	Convexity Mean
No treatment	120	11.43	0.267	0.342	0.638
2 minutes agitation, collected at P1	99	12.31	0.287	0.323	0.646
2 minutes agitation, collected at P2	104	12.62	0.262	0.357	0.634
2 minutes agitation, collected at P3	108	12.04	0.278	0.343	0.642
4 minutes agitation, collected at P1	117	11.20	0.262	0.366	0.637
4 minutes agitation, collected at P2	96	13.42	0.301	0.318	0.653
4 minutes agitation, collected at P3	94	12.78	0.294	0.329	0.649
Standard deviation	3.410	6.00	0.132	0.157	0.118

Table 19 Size and shape of potato particles .

Sample Name	# Particles per frame	CE Diameter Mean (mm)	Circularity Mean	Elongation Mean	Convexity Mean
No treatment	141	10.96	0.757	0.259	0.966
2 minutes agitation, collected at P1	213	9.70	0.740	0.284	0.962
2 minutes agitation, collected at P2	194	9.88	0.756	0.278	0.963
2 minutes agitation, collected at P3	229	9.47	0.740	0.289	0.957
4 minutes agitation, collected at P1	178	10.02	0.763	0.267	0.963
4 minutes agitation, collected at P2	186	9.92	0.777	0.264	0.968
4 minutes agitation, collected at P3	195	9.53	0.746	0.274	0.960
Standard deviation	6.423	2.76	0.087	0.139	0.173

Appendix E: Change in Size and Shape of Sample Particles

Highlighted in red – significant %change at 95% confidence level

Effect of agitation

Table 20 %Change on particle size and shape due to agitation.

Particle	Agitation time	% Change in Size and Shape			
		CE diameter	Circularity	Elongation	Convexity
Carrots	2 min	-3,18%	-3,15%	3,40%	-1,13%
Mango	2 min	7,63%	7,49%	-5,56%	1,25%
Potato	2 min	-11,56%	-2,25%	9,65%	-0,41%
Carrots	4 min	1,88%	2,40%	-5,66%	0,22%
Mango	4 min	-2,01%	-1,87%	7,02%	-0,16%
Potato	4 min	-8,64%	0,79%	3,09%	-0,31%

Effect of pump

Table 21 %Change on particle size and shape due to pump.

Particle	Agitation time	% Change in Size and Shape			
		CE diameter	Circularity	Elongation	Convexity
Carrots	2 min	11,42%	6,06%	-23,11%	0,79%
Mango	2 min	2,52%	-8,71%	10,53%	-1,86%
Potato	2 min	1,85%	2,12%	-2,20%	0,07%
Carrots	4 min	1,93%	6,21%	-9,17%	1,90%
Mango	4 min	19,74%	14,89%	-13,11%	2,51%
Potato	4 min	-1,00%	1,80%	-1,14%	0,51%

Effect of restriction pipe

Table 22 %Change on particle size and shape due to restriction pipe.

Particle	Outlet particle concentration	Agitation time	% Change in Size and Shape			
			CE diameter	Circularity	Elongation	Convexity
Carrots	48%	2 min	-3,45%	-1,81%	17,71%	-0,11%
Mango	42%	2 min	-4,54%	6,11%	-3,92%	1,26%
Potato	48%	2 min	-4,07%	-2,07%	4,05%	-0,59%
Carrots	20%	4 min	0,71%	-4,05%	9,62%	-1,10%
Mango	21%	4 min	-4,73%	-2,45%	3,40%	-0,66%
Potato	19%	4 min	-3,89%	-3,95%	3,81%	-0,82%

Effect of the processing

Table 23 %Change on particle size and shape due to the overall processing.

Particle	Agitation time	% Change in Size and Shape			
		CE diameter	Circularity	Elongation	Convexity
Carrots	2 min	4,15%	0,87%	-6,42%	-0,45%
Mango	2 min	5,34%	4,12%	0,29%	0,63%
Potato	2 min	-13,59%	-2,25%	11,58%	-0,93%
Carrots	4 min	4,58%	4,35%	-6,08%	1,00%
Mango	4 min	11,79%	9,98%	-3,86%	1,67%
Potato	4 min	-13,07%	-1,45%	5,79%	-0,62%

Appendix F: Sieving Analysis

Table 24 Particle size distribution (mass based) of carrot particles with 4 minute agitation.

Sieve size, mm	Weight of particles, g	%Particles retained
P0 – no treatment		
8.0	252.60	74.84%
5.6	62.46	18.51%
2.8	15.78	4.68%
1.0	6.66	1.97%
Total	**337.5**	**100.00%**
P1 – samples with agitation treatment		
Sieve size, mm	Weight of particles, g	%Particles retained
8.0	258.58	75.82%
5.6	60.68	17.79%
2.8	14.56	4.27%
1.0	7.22	2.12%
Total	**341.04**	**100.00%**
P2 – sample with agitation and pumping treatments		
Sieve size. mm	Weight of particles	%Particles retained
8.0	278.6021	79.80%
5.6	51.09	14.63%
2.8	12.31	3.53%
1.0	7.14	2.05%
Total	**349.14**	**100.00%**
P3 – sample with agitation, passing through pump and restriction pipe treatments		
Sieve size. mm	Sieve size. mm	Sieve size. mm
8.0	264.4702	75.79%
5.6	62.66	17.96%
2,8	14.40	4.13%
1.0	7.40	2.12%
Total	**348,93**	**100.00%**

Table 25 Particle size distribution (mass based) of mango particles with 4 minute agitation.

P0 – no treatment		
Sieve size, mm	**Weight of particles, g**	**%Particles retained**
11.3	100.96	68.58%
8.0	37.11	25.21%
5.6	6.78	4.61%
2.0	2.36	1.60%
Total	147.21	**100.00%**
P1 – samples with agitation treatment		
Sieve size, mm	**Weight of particles, g**	**%Particles retained**
11.3	91.96	57.0%
8.0	49.33	31.0%
5.6	14.95	9.0%
2.0	5.20	3.0%
Total	161.44	**100.00%**
P2 – sample with agitation and pumping treatments		
Sieve size. mm	**Weight of particles**	**%Particles retained**
11.3	114.32	64%
8.0	45.82	26%
5.6	11.62	7%
2.0	6.97	4%
Total	178.73	**100.00%**
P3 – sample with agitation, passing through pump and restriction pipe treatments		
Sieve size. mm	**Sieve size. mm**	**Sieve size. mm**
11.3	83.85	50%
8.0	58.71	35%
5.6	16.24	10%
2.0	8.98	5%
Total	167.78	**100.00%**

Table 26 Particle size distribution (mass based) of potato particles with 4 minute agitation.

P0 – no treatment		
Sieve size, mm	Weight of particles, g	%Particles retained
8.0	265.11	86.33%
5.6	27.10	8.82%
2.8	9.29	3.03%
1.0	5.60	1.82%
Total	**307.1**	**100%**
P1 – samples with agitation treatment		
Sieve size, mm	Weight of particles, g	%Particles retained
8.0	253.23	78.34%
5.6	47.83	14.80%
2.8	16.47	5.10%
1.0	5.72	1.77%
Total	**323.25**	**100%**
P2 – sample with agitation and pumping treatments		
Sieve size. mm	Weight of particles	%Particles retained
8.0	263.85	82.83%
5.6	37.77	11.86%
2.8	11.28	3.54%
1.0	5.66	1.78%
Total	**318.56**	**100%**
P3 – sample with agitation, passing through pump and restriction pipe treatments		
Sieve size. mm	Sieve size. mm	Sieve size. mm
8.0	264.44	83.88%
5.6	32.34	10.26%
2.8	12.04	3.82%
1.0	6.44	2.04%
Total	**315.26**	**100%**

Appendix G: Preliminary Experiments on Mechanical Tests

The particles are characterized according to their mechanical properties such as texture profile which is measured at the elastic limit of the particle and the bio-yield stress. The tests are done using the Stable Micro Systems TA.XT2, or commonly known as texture analyzer. Exponent software is used for the data gathering and analysis.

Calibration Procedure

Before doing any of the tests, the apparatus should be calibrated. From the tool bar menu of the Exponent software, 'T.A.' tab is clicked, then 'Calibrate', and 'Calibrate Force'. It is important that the texture analyzer's table and loadcell are free from any material. The installed loadcell capacity is also identified – in this case, the apparatus has 5 kg loadcell capacity, and the calibration weight is 2000 grams (g). A window showing that the calibration is complete should be displayed before removing the weight from the calibration platform.

The probe height is also required to be calibrated when measuring parameters in % strain, recording the height of the product during the test, using a button trigger, and starting each test from the same position. From the tool bar menu of the Exponent software, 'T.A.' tab is clicked, then 'Calibrate', and 'Calibrate Height'. It is also important that during calibration, the texturometer table is clear from any sample, and the position of the probe should be as close to the base. The return distance and speed is set to 100 cm and 5 mm/sec respectively. A window showing that the calibration is successful should be displayed.

Setting the test parameters for mechanical tests

Compression test involves application of axial force to the sample particle wherein the probe has higher contact area than the sample, while in puncture test, the probe's contact area is smaller compared to the sample so it can penetrate. In this study, a cylinder with 36 mm diameter is used for compression tests, while puncture probes of 2 mm and 5 mm are used for puncture tests.

Since the identified phases of deformation that are dealt with are in the early phase, it is expected that the % strain to be applied are low. Initially, the particles are tested under 2%, 10% and 20% strains. Probe speed and trigger force are also important parameters in compression and puncture tests. With the given % strains used, these parameters could also vary.

Pre-test speed and post-test speed are the speeds of the probe wherein it is not in contact with the sample particle. This is set to be as close to the test speed in order to avoid sudden acceleration or deceleration of the probe, as supported by the recommendations by Khanh and Glasgow (2012), and Li et al. (2017). Nevertheless, it is more critical to focus on the test speed. By principle, lower probe speed and lower trigger force should be applied to lower strain to avoid pre-compression of sensitive particles before the test compression. For example, if 5 g trigger force is applied to very sensitive particles like blueberry and raspberry, the particle is already compressed before the measurement during the test compression is done. This could lead to inaccurate measurement of parameters. On the other hand, if the trigger force is relatively too low for more sturdy particles, the trigger force could only be caused by very small uneven surface of the particle. It is important then that during compression test, especially in small strains, the apparatus should be free from any movement, vibration or from any causes of small trigger forces. This issue can be attributed to the fact that the load cell capacity of the texture analyzer is very high (5000 g) relative to the small forces involved in very low strains, low test speed and trigger force. The test parameters of the double compression (texture profile analysis) is shown in Table 27.

Table 27 Test parameters of double compression test (texture profile analysis) at different %strains.

| Test setting parameters	%Strain		
	2%	10%	20%
Probe type	36 mm cylinder probe	36 mm cylinder probe	36 mm cylinder probe
Number of cycles	2	2	2
Pre-test speed, mm/s	0.50	1.0	1.0
Test speed, mm/s	0.20	0.50	1.0
Post-test speed, mm/s	0.50	1.0	2.0
Trigger force, g	1.0	2.0	2.0

The strain applied is in terms of percentage (%) of the height so that it would be applicable to all particles. Considering elastic limits of very sensitive and soft particles, the %strain that should be applied are very low. With 2% strain applied, the particles exhibited around 100% springiness which means that the particle is not deformed at all, a clear indication of the elastic phase (see Table 28). Application of 10% strain gives approximately 80% springiness of the sample particles, while 20% strain gave springiness values less, but close to 80%. At this point, the particle is deformed, but in temporary state and can regain its structure through time.

Table 28 Springiness of selected particles at different % strains.

	Dimensions	Springiness (%) at 2% strain	Springiness (%) at 10% strain	Springiness (%) at 20% strain
Thawed diced carrots	1x1 cm	89.55 ± 3.92	82.45 ± 9.05	76.49 ± 7.56
Canned peach cut in cubes	1x1 cm	93.62 ± 8.13	88.78 ± 3.62	82.43 ± 2.00
Thawed blueberry	0,6 cm height	99.19 ± 0.98	88.40 ± 11.64	74.89 ± 10.18

However, the graph of the double compression with 2% strain showed that peak force is very close to the trigger force. Figure 55 shows the graph of TPA of thawed diced carrots at different %strains. The force measurements in very low %strain could only be from the variations in the surface of the sample particle. The intense variations is shown in sensitive particles like blueberry. Consequently, 2%

strain is not considered in the measurement of texture profile of particles. This method might not be suitable for measuring very sensitive fruit sample such as berries. There is developed method for evaluating the firmness of such tissue, for example, hand held portable instrument developed for evaluating berries (Timm et al., 1993). Many other methods and instruments have been developed to measure firmness in small fruits such as blueberries (Slaughter & Rohrbach, 1985) cherries (Lustig and Bernstein, 1987); strawberries (Ourecky & Bourne, 1968).
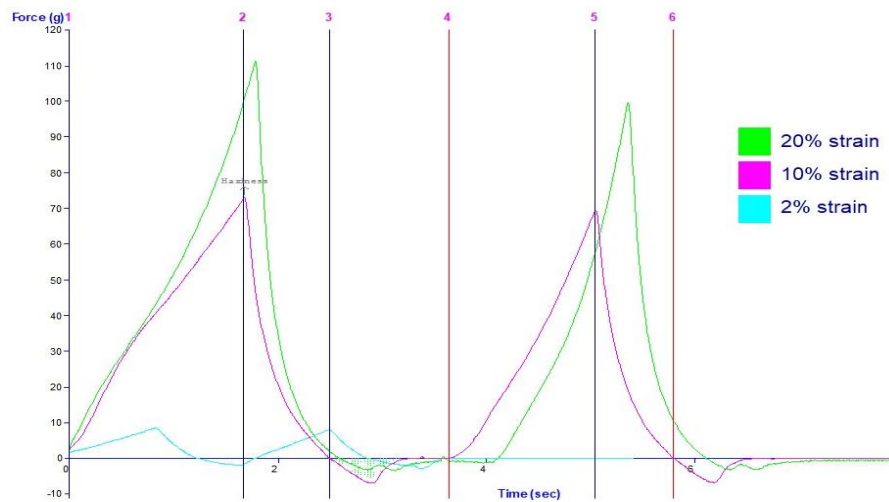
Figure 55 Time vs force graph of thawed carrots cube (1x1cm) at different strains.

86

Appendix H: Preliminary Experiments on the Pilot Scale Experiment

The focus of the experiment is to determine the effect of restriction pipe to the size and shape of the particles. There is another concomitant simulation study being conducted on the behavior of particles on a restriction pipe. Results of which are to be related to this study. There are also 3 available restriction pipes available – 16 mm inner diameter, 26 mm inner diameter and 36 inner diameter.

Figure 56 Restriction pipes.

Preliminary experiments is done to determine settings to minimize the effect of other different factors like flow rate, viscosity of suspending medium, particle concentration and agitation time. Given the availability, cost effectiveness and handling of canned diced potato, it is used for the initial test runs.

Measurement of viscosity

Bohlin Visco 88 viscometer was used to measure the viscosity of the fluid with the following steps:

1. The aliquot CMC fluid sample are obtained from point 1 in the pilot scale experiment.
2. Fifteen (15) ml of sample are filled in the outer cylinder (diameter 27.5 mm) then wait for the temperature of the sample to reach approximately 17-18 C.

Figure 57 Cup containing the liquid sample for viscosity analysis.

3. In prior to the assembling of inner cylinder and outer cylinder, the inner cylinder are attached to the viscometer apparatus, then the outer cylinder which contains the sample is assembled to the inner cylinder.
4. Switch the apparatus to position 2.
5. Start running the instrument from system 1, then wrote down the measurement output such as actual temperature, shear rate, viscosity and momentum and shear stress.

Figure 58 Measurement of viscosity using Bohlin viscometer.

6. It should be noted that the fluid sample should have the temperature approx. 20 C during the entire measurement.
7. Then, the viscosity of fluid sample at shear rate of 100 s-1, 20ºC is calculated by extrapolation from the shear rate and shear stress curve using n and k value.

Preparation of the liquid medium and setting of lobe pump frequency and flow rate

With 3 target test flow rates, the frequency of the pump is determined by running three fluids with different viscosities. Table 29 presents the three types of viscosities and their formulation.

Table 29 Viscosities of different CMC mixture as suspending medium of the particles.

Categorical viscosity	Target viscosity, (mPas)	Formulation (%w/w)	Actual viscosity (mPas, at 20ºC, 100 s^{-1})	Target flow rate		
				1 m^3/h	2 m^3/h	3 m^3/h
				Pump frequency, Hz		
High viscous	2×10^3	2% CEKOL CMC 30000 in water	1695	3,5	7,0	10,0
Medium viscous	2×10^2	2% CEKOL CMC 700 in water	265	3,5	7,0	10,0
Non-viscous	1	100% water	1	5,0	8,0	11,0

On a 500-liter batch of liquid medium, 2% mixture of CEKOL carboxymethyl cellulose (CMC) 30000 molecular weight (MW) and water is prepared to test for approximately 2000 cp suspending medium, while 2% of CMC 700 in water is also used to test for approximately 200 cp suspending medium. The mixture is prepared under vacuum (0.6 barrs absolute pressure), with 60% setting of the high shear mixer and 100% setting of agitator for approximately 2 minutes. The temperature of the mixture during mixing is maintained at the range of 15 ºC to 18 ºC. Aliquot samples are analyzed for viscosity measurement using Bohlin Visco. The mixture is then pumped into the inlet tank by centrifugal pump.

The flow rate is estimated by determining the time to obtain approximately 7 kg of liquid medium using a bucket. The sample is weighed, to calculate for the flow rate using the formula below:

Equation 6 $\text{Flow rate}, \dfrac{m^3}{h} = \dfrac{(\text{weight of sample obtained,kg})}{(\text{time,s})} \times \dfrac{1\ m^3}{1000\ kg} \times \dfrac{3600\ s}{1\ hr}$

Viscosity of liquid medium

Canned diced potato particles suspended in different viscosities of medium – high viscous (1695 mPa.s), and non viscous (1 mPa.s) - are tested in the set up rig using 25 mm inner diameter dummy restriction pipe. The calculated particle concentration in the task is set to 10% (w/w) on a 500-liter batch size. The objectives are to qualitatively asses the effect of these extreme viscosities on the particles, observe the breakage due to viscosity, dispersion of particles in the tank, and the practicality in sampling method.

The issues with using the high viscous medium is that it took more agitation time to evenly disperse the particle in the tank. At least 5 minutes agitation time provides well dispersed particles in the tank (see Figure 59).
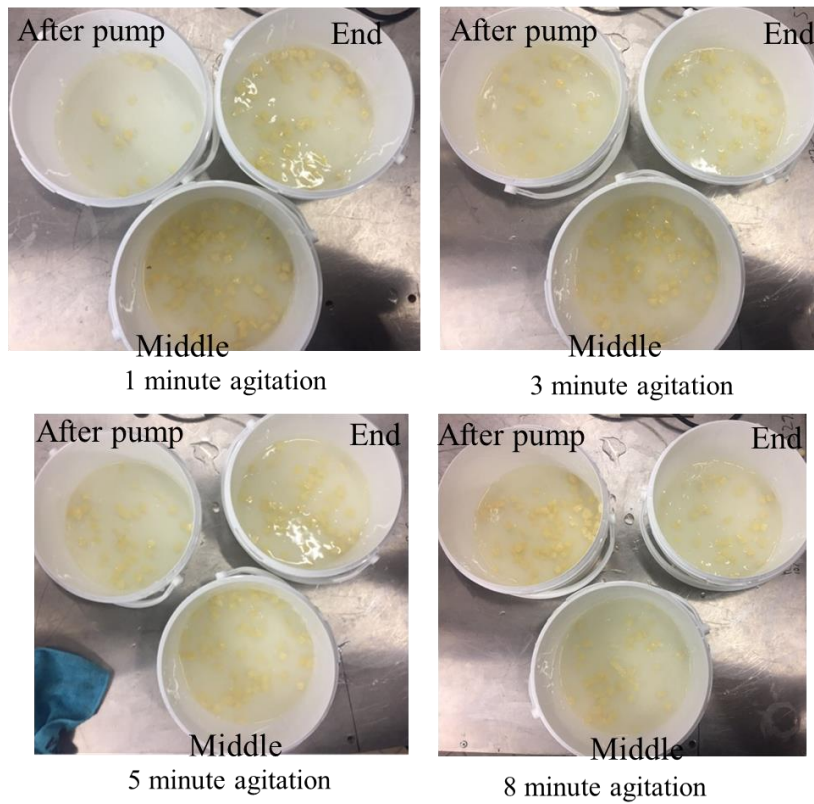
Figure 59 Difference in particle dispersion (in high viscous medium) from different sampling points at different agitation time.

However, the particle in low viscous medium is easily destroyed by the agitator by which its integrity changed significantly (see Figure 59). From the cube shape, particles become more spherical. Sampling is also challenging because particles sinks very fast.
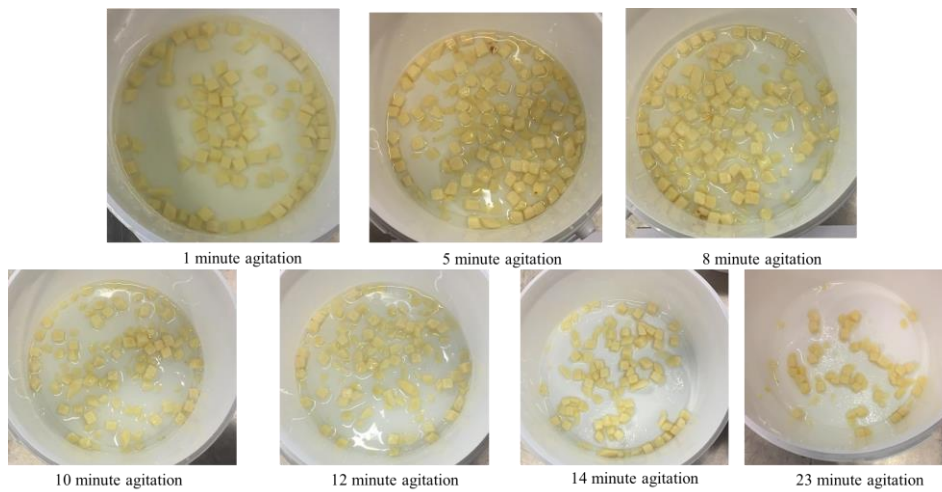
Figure 60 Effect of agitation time to particles in non viscous medium.

In contrast, the potato particles in high viscous medium slightly change their appearance (see Figure 60). There are small bits of broken potato particles but the 'cubeness' of the particles is still retained unlike in the particles suspended in non viscous medium. The effect of agitator is more pronounced in the particles in non viscous medium. In other words, the particles could already be broken before it passes through the restriction pipe

No agitation

8 minutes agitation

10 minutes agitation

12 minutes agitation
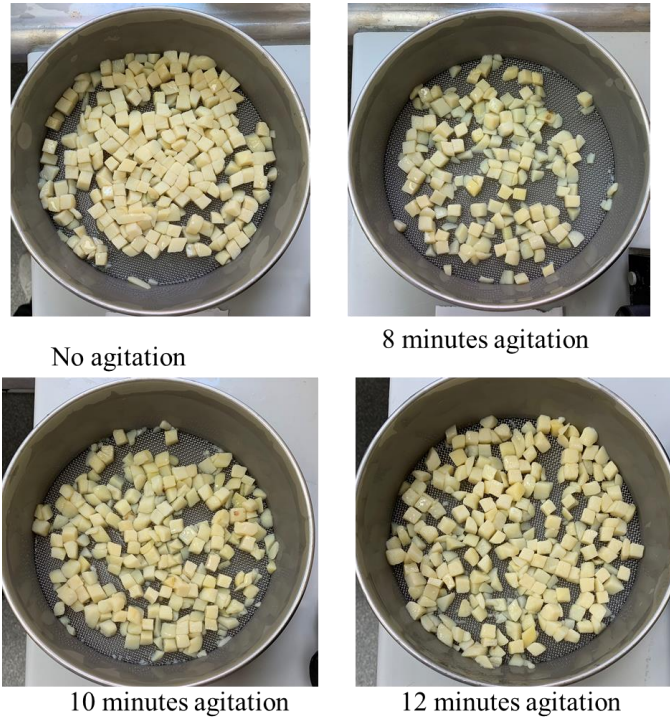
Figure 61 Particles at different agitation time in high viscous medium.

On the other hand, by subjective evaluation, the appearance of particles in high viscosity medium obtained from Point 2 and Point 3 did not exhibit difference; thus, the rig did not affect the particles in a highly viscous medium (see Figure 61).

Particles in non viscous
medium from Point 2

Particles in non viscous
medium from Point 3

Particles in viscous
medium from Point 2

Particles in viscous
medium from Point 3

Figure 62 Particles in different viscosities of medium agitated for 5 minutes, and sampled before restriction rig (Point2) and after restriction rig (Point 3).

The summary of the issues in using high viscous and non viscous medium are presented in Table 30.

Table 30 Comparison between using high viscous and non-viscous medium.

Factors	High viscous medium (2000 cp)	Low viscous medium (1 cp)
Agitation time to disperse particles	5 minutes	10 seconds
Sampling at the tank	Particles are well dispersed	Challenging due to particles sinking fast
Sinking of particles	Slower	Faster
Breakage due to agitation	Less	High
Effect of different flow rates	Low or high flow rate ➔ no significant destruction	high flow rate ➔ significant destruction
Particles after passing through pump and contraction	No difference	Particles are already broken due to agitation

The tested viscosities are in the extreme side of actual viscosities used as suspending medium of particles. In order to control the qualitatively significant effect of the other factors to the particles, it is agreed to use a medium viscosity (200 mPa.s), 3 m^3/h flow rate, to adapt a more realistic settings in food processing. A target particle concentration of 30% is also desired.
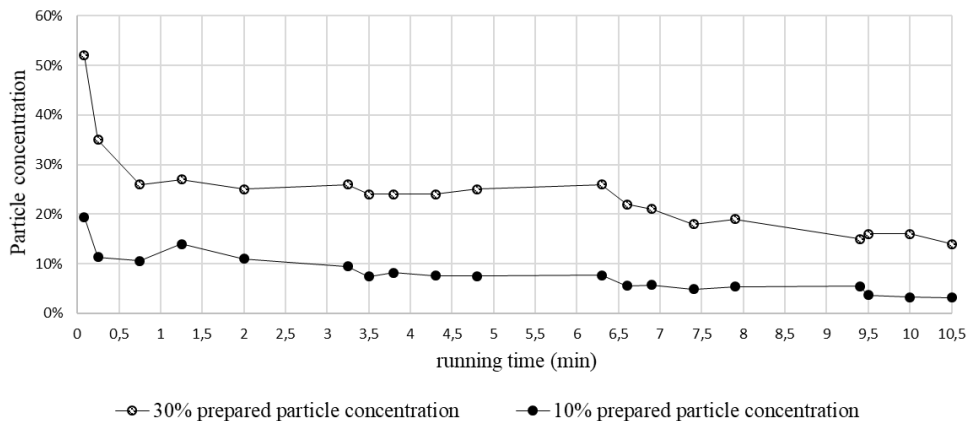
Particle concentration

Aside from the several issues raised in using different extremes of viscosities as medium, another phenomenon observed in the run is the varying particle concentration. The general observation is that, the particle concentration in the output (Point 3) during the initial running time is very high, and then stabilizes. This is also considered in the succeeding run of the experiments.
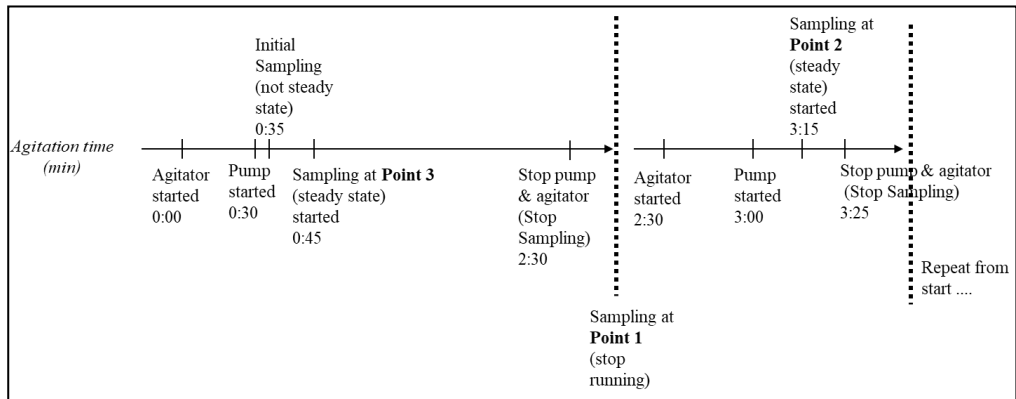
Figure 63 Timeline in running the experiment.

Applying the experimental set up concluded in the previous experiment, 10% particle concentration (w/w) is prepared in order to monitor the changes in concentration through time. The viscosity of the medium is set to approximately 200 mPa.s, and the flow rate is 3 m^3/h. The particle concentration is done by collecting sample at the outlet (P3) for 4 seconds to fill a 2-liter bucket every 30 seconds for 2 minutes. The samples are then weighed to calculate for the flow rate, and particle concentration. The particles are washed and drained using 2 mm sieve for 3 minutes until no dripping liquid. The following formula is used in calculating for the particle concentration:

Equation 7 $\text{Particle concentration, }\% = \dfrac{\text{Weight of ished and drained particles,kg}}{\text{Weight of sample (liquid+particles),kg}} \text{ x } 100$

Figure 64 Monitoring the particle concentration during running time.

It can be observed that the initial particle concentration of the prepared mixture is at 20% and decreases through time until it reached 4% after 555 seconds (9 minutes, 15 seconds) of running time. This phenomenon happened because the lobe pump has very high suction pressure causing bulk of particle to move forward the tank to the pump during the initial run, and though there is constant agitation during the test run. Figure 65 also shows the particle concentration of the carrots, mango and potato during the run.
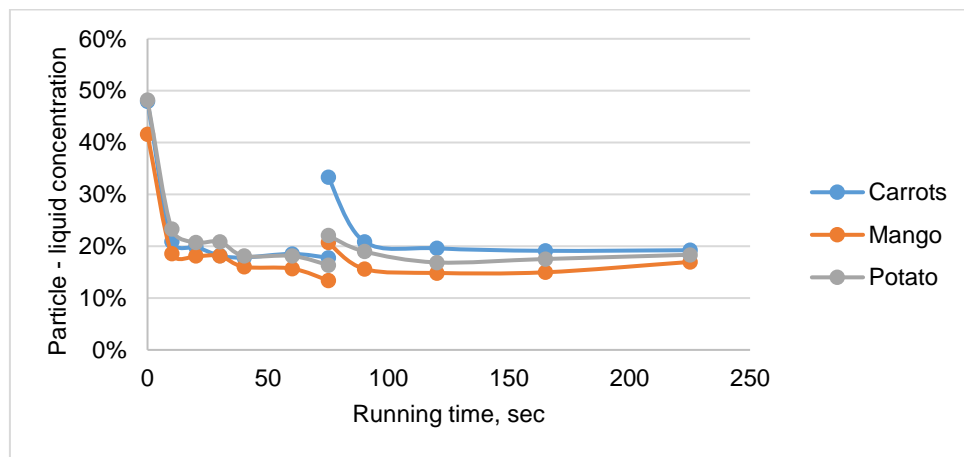

Figure 65 Monitoring the particle concentration during running time.

Effect of agitation time

From the previous preliminary experiments, it has been known that agitation has effect on the physical properties of the particles. Particles tend to exhibit breakage when subjected to prolonged agitation. However, the goal of the experiment is to minimize the breakage caused by other factors, in order to see the effect of the restriction pipe to the particles.
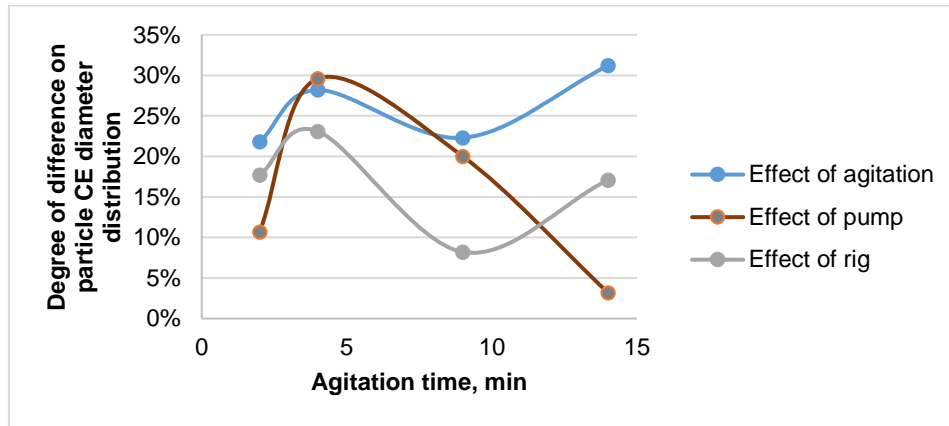
Figure 66 Degree of difference on particle size distribution of particles in different processing treatments.

Particles in medium viscous medium (approximately 25% concentration, w/w) are agitated in different duration, and samples are collected for analysis. It shows that the particle diameter distribution exhibits more change after agitation, than passing through restriction pipe. In other words, particles might have been broken already due to agitation before it passes through the restriction pipe, thereby reducing the effect of the latter to the particles. On the other hand, the degree of difference in particle diameter distribution as the effect of pump shows fluctuating values. It should be noted though that the analysis is from one trial, and only aimed to give indicative comparison of effect of agitation and effect of pipe. In this regard, it is concluded to minimize the agitation time, to 2 minutes, for the trials on the particles with different mechanical properties.

In conclusion, based on the results of the preliminary test, the control variables considered in the experiment with carrots, mango and potatoes are the following:

- Medium viscosity of fluid medium 200 mPa.s (at 20 C, 100 s-1)
- Fluid flow rate of 3 m3/h (10 Hz pump's motor frequency)
- Particle-liquid concentration of 20-30% w/w
- Restriction pipe inner diameter of 16 mm for particles with 1x1x1 cm dimension, and restriction pipe with 26 mm inner diameter for particles with 1.7x17x1.7 cm dimension
- 2 minutes agitation time

# Appendix I: Preliminary Experiments on Morphological Analysis

Particle dispersion

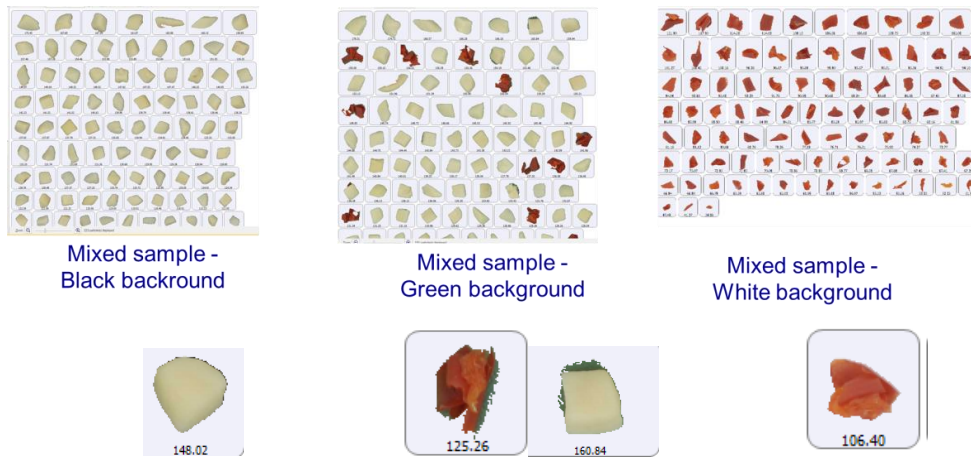The important considerations in the sample dispersion are the following:

- *Proper frame background* – The background should provide good contrast to the particles for it to be easily and accurately analyzed.
- *Standard amount of particles in one frame* – The particles should be properly dispersed in the frame for analysis. Crowded particles give a risk of overlapping and attaching which affects the results of analysis. For better comparison of different particles, the number of particles that should be analyzed should also be as close as possible.
- *Frame dimension and frame placement* – The dimension and placement of the frame should fit into the apparatus. For one analysis run, the sample dispersion is limited into one dimension of the frame. In effect, fewer particles are analyzed if the particle dimensions are bigger.

First of all, appropriate background color of the particle for image capturing should be chosen. The goal is to have good contrast of the particle and background so that the former will effectively float in the image analysis. In the preliminary experiment using mixture of potato and red bell pepper, it is found that black and white backgrounds provide best quality image of the particles, though they cannot detect both types of particles. Red bell pepper cannot be detected if they are dispersed in black background, while potatoes can be detected. On the other hand, potatoes cannot be detected when dispersed in white background, while red bell peppers can. For both of the different types of particles to be detected, green background is needed; however, the particle images are not of good quality.
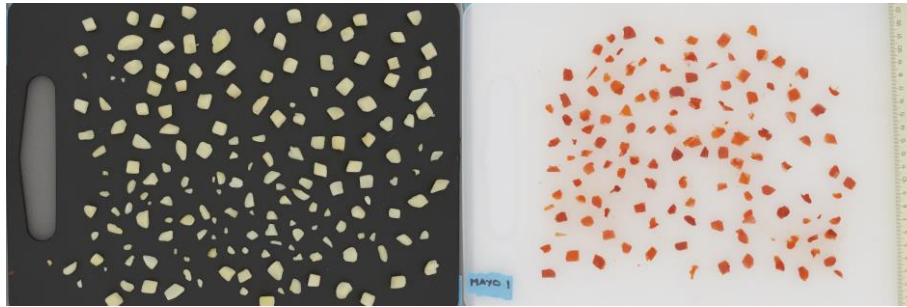
Figure I1 (Left) Potato (yellow) particles dispersed in black frame board; (Right) Red paprika particles dispersed in white frame board.

Mixed sample -
Black backround

Mixed sample -
Green background

Mixed sample -
White background

148.02

125.26

160.84

106.40

Figure 67 Potato and red bell pepper particle are precisely detected with black and white background respectively (left and right) while they are poorly detected in green background (center).

Table 31 Suggested background color for various particle colors.

Black	White
Yellow (potato, mango)	Red (paprika, strawberry, raspberry)
Orange (carrots)	
Cream (oats, barley)	Blue (blueberry)
White (rice)	Green (olives)
	Black (olives)
	Orange (carrots, tomato)

In order to analyze the change in size and shape parameters, the respective particle size distribution graphs can be used and compared. In the '*Comparison tab*', he Morphologi 4-ID provides frequency distribution curve and the corresponding

100

undersize (or cumulative distribution) curve of each of the parameters measured. A dendrogram and trend pot, based on the distribution curve are also presented in comparing two or more samples. Dendrogram is a diagram that can show the degree of difference of two samples. The x-axis indicates the variation between records. With the highest value equal to 1, the higher the value of record difference, the more divergent range of parameter values. On the other hand, when the value is close to 0, the more similar the samples are. Trend plot shows the mean values of the parameter being measured, and their relative 'distance' to each other. It can also show the direction of the change if increasing or decreasing.
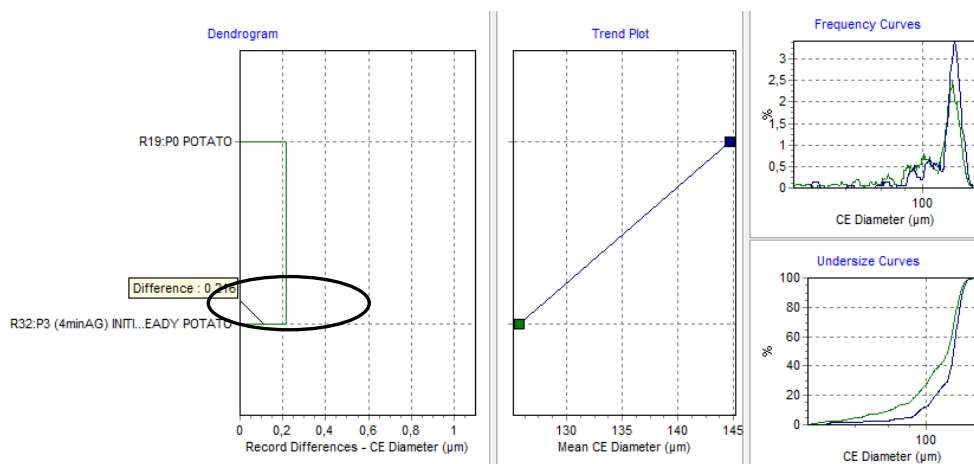

Figure 68 Comparison tool for the particle parameters used in Morphologi 4-ID.

In this proposed method, the degree of change in size and shape of the particles is interpreted on the basis of the degree of difference of the frequency curves of the samples being compared. As an example of potato samples shown in Figure I3. R19:P0 Potato is the particle profile before treatment, and R32:P3 (4min AG) is the sample profile record after treatment. The degree of 'change' in CE diameter is 0,216 or 21,6%, and the trend is decreasing. It means that the potato particles changed this parameter by 21,6% by in generally decreased value.

Variation

The imaging method analyses the particle shape and size from the top view (2D) because the camera is installed above the particle sample. Consequently, if the sample particles are oriented and arranged differently, the image analysis will still detect variation in size and shape to some extent. This is illustrated in Figure 68.

101
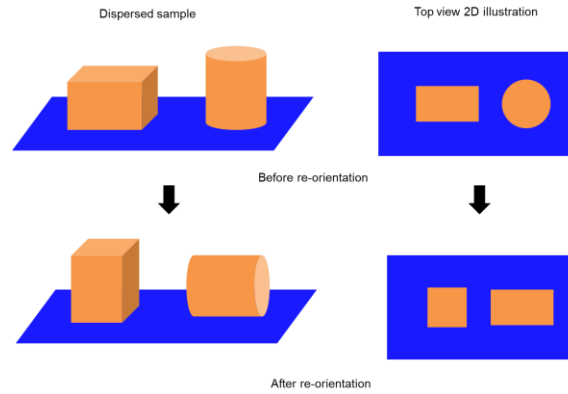
Figure 69 Illustration in the change in 2D image after re-orientation of the particles.

Replication by multiple sampling is statistically the best way to identify this variation. More than one sample is obtained from the same batch of treatment. In this multiple sampling, the variability is from the inhomogeneity of the particles suspended in the entire batch. In other words, there will be more than one sample per treatment for image capturing and analysis.